REPORT 951

USE OF SOURCE DISTRIBUTIONS FOR EVALUATING THEORETICAL AERODYNAMICS OF THIN FINITE WINGS AT SUPERSONIC SPEEDS

By JOHN C. EVVARD

SUMMARY

A series of publications on the source-distribution methods for evaluating the aerodynamics of thin wings at supersonic speeds is summarized, extended, and unified. Included in the first part of this report are the derivations of: (a) the linearized partial-differential equation for unsteady flow at a substantially constant Mach number; (b) the source-distribution solution for the perturbation-velocity potential that satisfies the boundary conditions of tangential flow at the surface and in the plane of the wing; and (c) the integral equation for determining the strength and the location of sources to describe the interaction effects (as represented by upwash) of the bottom and top wing surfaces through the region between the finite wing boundary and the foremost Mach wave.

The second part of the report deals with steady-state thin-wing problems. The solution of the integral equation for upwash is presented and applied in numerous examples to obtain the velocity potential and loading for several families of curved plan boundary wings. The concept and the evaluation of the suction force along subsonic leading edges are included. The loading associated with the vortex sheet (or discontinuity in sidewash) behind subsonic trailing edges is described and evaluated for wings satisfying the Kutta-Joukowski condition along subsonic trailing edges.

The third part of the report approximates the integral equation for unsteady upwash and includes a solution of the approximate equation. Expressions are then derived to evaluate the load distributions for time-dependent finite-wing motions.

INTRODUCTION

The analysis of the aerodynamic effects in the vicinity of thin wings at supersonic speeds can be simplified by linearizing the partial-differential equation of a compressible fluid. This linearization is accomplished by assuming that the perturbation-velocity components associated with the wing are small in comparison to the velocity of sound and that the free-stream Mach number is sufficiently different from unity. Solutions to the linearized partial-differential equation of the flow that satisfy the boundary conditions in the vicinity of the wings must then be found. The flow must be tangent to the wing at its surface and no disturbances can propagate ahead of the forward Mach envelope of the wing.

Numerous approaches lead to solutions of the steady-state thin-wing problems. For two-dimensional wings, the Ackeret theory (reference 1) may be applied to evaluate both lift and wave-drag coefficients. The line-source and point-source methods of references 2 and 3 may be effectively used to obtain solutions for the aerodynamic coefficients of three-dimensional wings if the flow on the bottom and top surfaces are independent. This condition holds for symmetric wings at zero angle of attack and for wing regions influenced only by supersonic leading edges. (That is, the component of the flow normal to the edge is supersonic.) Wing regions influenced by upwash in the flow field between the wing boundary and the foremost Mach lines, however, must be excluded.

The effects of the upwash field may be evaluated for wings of straight-line plan boundaries by the conical-flow method of references 4 to 6. The doublet-distribution method of reference 7, as applied to the triangular wing, inherently includes the effect of upwash fields and may conceivably be extended to obtain quite general solutions for thin three-dimensional wings. An approach to this extension and a synthesis of the various methods as special cases of a general theory are included in references 8 and 9. The application of horseshoe vortices for solving the finite-wing problem is included in reference 10.

The time-dependent aerodynamic effects (including the transient disturbances of gusts, changes in angle of attack, skin vibration, and flutter) near thin wings at supersonic speeds are more difficult to obtain. A number of investigators have studied two-dimensional time-dependent flows over thin wings; these flows are generally included as special cases of the theory of reference 11. The method of reference 11 is similar to the steady-state method of reference 3 and includes three-dimensional or finite-wing solutions so long as the aerodynamic effects of the bottom and top wing surfaces are independent.

If the upwash in the flow field between the wing boundary and the foremost Mach wave could be evaluated, the methods of references 3 and 11 could be applied to determine the aerodynamic coefficients in the flow field of lifting three-dimensional thin wings at supersonic speeds. This approach to the evaluation of the upwash field implicitly or explicitly has led to the methods of solution developed at the NACA Lewis laboratory and presented in references 12 to 19. The work included in these reports is extended and unified herein.

The fundamental equations are derived in general form in the first part of the report. The applications of the integral equation for determining upwash to obtain the flow over

wing surfaces for time-independent and time-dependent problems are included in the second and third parts, respectively. Specific examples are included at pertinent points throughout the discussion.

I—INTEGRAL EQUATION FOR UPWASH

In order to unify the discussion, parts of the fundamental treatment of reference 11 are repeated. A similar discussion for steady-state potentials is given in reference 3. The presentation includes the derivations of: (1) the time-dependent, linearized partial-differential equation for the perturbation-velocity potential of an ideal fluid, (2) the fundamental solution that will satisfy the boundary conditions on the wing, and (3) the integral equation for the upwash over the wing plan boundaries.

Differential equation.—The linearized Euler's equations for a compressible fluid may be written

$$\left.\begin{aligned}\frac{\partial^2\varphi}{\partial x\partial t}+U\frac{\partial^2\varphi}{\partial x^2}&=-\frac{1}{\rho_0}\frac{\partial p}{\partial x}\\ \frac{\partial^2\varphi}{\partial y\partial t}+U\frac{\partial^2\varphi}{\partial x\partial y}&=-\frac{1}{\rho_0}\frac{\partial p}{\partial y}\\ \frac{\partial^2\varphi}{\partial z\partial t}+U\frac{\partial^2\varphi}{\partial x\partial z}&=-\frac{1}{\rho_0}\frac{\partial p}{\partial z}\end{aligned}\right\}\tag{1}$$

where

p static pressure
t time
U free-stream velocity
x, y, z Cartesian coordinates (free stream parallel to x-axis)
ρ_0 free-stream density
φ perturbation-velocity potential (based on free-stream velocity)

(For convenience, a complete list of symbols is included in appendix A.)

When equations (1) are multiplied by dx, dy, and dz, respectively, added, and integrated, the result is

$$\frac{\partial\varphi}{\partial t}+U\frac{\partial\varphi}{\partial x}+\frac{p}{\rho_0}=g(t)\tag{2}$$

where $g(t)$ is an integration constant at any given time.

The linearized continuity equation assumes the form

$$\frac{\partial\rho}{\partial t}+U\frac{\partial\rho}{\partial x}+\rho_0\left(\frac{\partial^2\varphi}{\partial x^2}+\frac{\partial^2\varphi}{\partial y^2}+\frac{\partial^2\varphi}{\partial z^2}\right)=0\tag{3}$$

or, because the speed of sound c is

$$c^2=\frac{dp}{d\rho}\approx c_0^2$$

equation (3) becomes

$$\left(\frac{\partial}{\partial t}+U\frac{\partial}{\partial x}\right)\frac{p}{\rho_0 c_0^2}+\frac{\partial^2\varphi}{\partial x^2}+\frac{\partial^2\varphi}{\partial y^2}+\frac{\partial^2\varphi}{\partial z^2}=0\tag{3a}$$

Elimination of $\frac{p}{\rho_0}$ between equations (2) and (3a) gives

$$(1-M^2)\frac{\partial^2\varphi}{\partial x^2}+\frac{\partial^2\varphi}{\partial y^2}+\frac{\partial^2\varphi}{\partial z^2}=\frac{1}{c^2}\frac{\partial^2\varphi}{\partial t^2}+\frac{2U}{c^2}\frac{\partial^2\varphi}{\partial x\partial t}-\frac{1}{c^2}\frac{dg}{dt}\tag{4}$$

where M is the free-stream Mach number and the subscript has been dropped from c.

Equation (4) is the required linearized partial-differential equation for steady or unsteady velocity potentials. If φ and g are independent of time, the Prandtl-Glauert equation results.

If the flow ahead of the body is uniform and undisturbed, the function $g(t)$, which is independent of position, will be constant (from equation (2)) and equal to $\frac{p_0}{\rho_0}$; the term $\frac{dg}{dt}$ will then contribute nothing to equation (4). Under these conditions, which are assumed for the rest of the analysis, equation (2) may be written

$$C_p=\frac{p-p_0}{\frac{1}{2}\rho_0U^2}=-\frac{2}{U}\left(\frac{\partial\varphi}{\partial x}+\frac{1}{U}\frac{\partial\varphi}{\partial t}\right)\tag{2a}$$

where C_p is the pressure coefficient.

A change of variable will convert equation (4) to a standard form of the wave equation. The transformations are

$$\left.\begin{aligned}x'&=x\\ y'&=\sqrt{1-M^2}\,y\\ z'&=\sqrt{1-M^2}\,z\\ t'&=(1-M^2)t+\frac{xM}{c}\end{aligned}\right\}\tag{5}$$

Equation (4) then becomes

$$\frac{\partial^2\varphi}{\partial x'^2}+\frac{\partial^2\varphi}{\partial y'^2}+\frac{\partial^2\varphi}{\partial z'^2}=\frac{1}{c^2}\frac{\partial^2\varphi}{\partial t'^2}\tag{6}$$

Basic solutions of equation (6) corresponding to spherical waves are

$$\left.\begin{aligned}\varphi&=\frac{1}{R'}f\left[-\frac{1}{\beta^2}\left(t'+\frac{R'}{c}\right)\right]\\ \text{and}\qquad\varphi&=\frac{1}{R'}f\left[-\frac{1}{\beta^2}\left(t'-\frac{R'}{c}\right)\right]\end{aligned}\right\}\tag{7}$$

where

$R'=\sqrt{x'^2+y'^2+z'^2}$

$\beta^2=M^2-1$

f arbitrary function representing a source strength

Garrick and Rubinow have shown (reference 11) that the basic solution for $M>1$ is obtained as the sum of equations (7). If this solution is transformed to a general point in the x, y, z space, each of the addends becomes a retarded potential in the basic solution of equation (4), which is

$$\varphi=\frac{1}{R}\left\{f\left[\xi,\eta,\zeta,\frac{t\beta^2c-(x-\xi)M-R}{\beta^2c}\right]+f\left[\xi,\eta,\zeta,\frac{t\beta^2c-(x-\xi)M+R}{\beta^2c}\right]\right\}\tag{8}$$

where ξ, η, and ζ are Cartesian coordinates of the source, and R is given by

$$R=\sqrt{(x-\xi)^2-\beta^2(y-\eta)^2-\beta^2(z-\zeta)^2} \tag{9}$$

Extended solutions of equation (8) may be obtained by integration with respect to any of the variables ξ, η, or ζ. For thin wings, the sources of the disturbances will lie in the plane of the wing, which may be defined by the relation $\zeta=0$. The immediate problem is to determine the strength of the source f in order to satisfy conditions of tangential flow on the surface of the wing, which in linearized theory is treated as though it were in the $z=0$ plane.

Fundamental solution for thin wings.—The impulses that the wing transfers to the fluid are primarily in the z-direction. This fact suggests that the strength of the source f is closely associated with the z component of the perturbation velocity $\frac{\partial\varphi}{\partial z}$. The value of $\frac{\partial\varphi}{\partial z}$ at each local point on the constraining wing surface is determined only by the local wing slope near that point.

The z component of the perturbation velocity obtained by differentiating the isolated source solution of equation (8) is

$$\frac{\partial\varphi}{\partial z}=-\frac{\beta^2 z}{R}\frac{\partial\varphi}{\partial R} \tag{10}$$

The wing dictates that $\frac{\partial\varphi}{\partial z}$ cannot be zero near $z=0$. Equation (10), however, indicates that $\frac{\partial\varphi}{\partial z}$ will be zero in the x,y plane except at points near $R=0$. (Infinite values of $\frac{\partial\varphi}{\partial R}$ are generally included in this condition.) The quantity R is nearly zero either close to the source, where $(x-\xi)$, $(y-\eta)$, and z are small, or on the boundary of the Mach cone from the source, where $(x-\xi)^2=\beta^2[(y-\eta)^2+z^2]$. As may be verified by direct calculation in specific examples, the second condition does not contribute to the value of $\frac{\partial\varphi}{\partial z}$ at the point $(x,y,0)$ on the constraining wing surface.

In the vicinity of the point $(x,y,0)$, the source strength per unit area assumes a mean value obtained by replacing ξ and η by x and y in the source strength f of equation (8). The velocity potential at point (x,y,z) associated with this substantially constant source distribution in the $z=0$ plane may be obtained by integration over the source area included in the forward Mach cone. The field of integration (fig. 1) is bounded by the curves $\xi=\xi_1$ and $(x-\xi)^2-\beta^2(y-\eta)^2-\beta^2z^2=0$ yielding the velocity potential

$$\varphi=2f(x,y,t)\int_{\xi_1}^{x-\beta z}d\xi\int_{\left[y-\frac{1}{\beta}\sqrt{(x-\xi)^2-\beta^2z^2}\right]}^{\left[y+\frac{1}{\beta}\sqrt{(x-\xi)^2-\beta^2z^2}\right]}\frac{d\eta}{\sqrt{(x-\xi)^2-\beta^2(y-\eta)^2-\beta^2z^2}}$$

$$=\frac{2\pi f(x,y,t)}{\beta}(x-\beta z-\xi_1) \tag{11}$$

For steady flows, this equation is the Ackeret value for the potential of an unswept two-dimensional flat plate and represents the contribution of the local point to the velocity potential near that point. Partial differentiation of equation (11) with respect to z gives

$$\frac{\partial\varphi}{\partial z}=w(x,y,t)=-2\pi f(x,y,t) \tag{12}$$

where w is the local z component of the perturbation velocity measured positively outward from the wing surface. The function f at an arbitrary point (ξ,η) is thus proportional to the z component of the perturbation velocity at that point. The fact that $\frac{\partial\varphi}{\partial z}$ from equation (12) is independent of ξ_1 illustrates that the sources along the Mach cone for which $R=0$ do not contribute to w. (Neither the basic solution of equation (8) nor its derivative, equation (10), is defined on the Mach cone. The integration, equation (11), of the basic source solution and the derivative, equation (12), of equation (11) are, however, defined functions. The order of integration and differentiation of the basic source solution to obtain equation (12) cannot be interchanged without special precautions.)

A condensation of the notation is advisable at this point. The time delays that occur in equation (8) can be denoted by τ_a and τ_b where

$$\left.\begin{aligned}\tau_a&=\frac{(x-\xi)M}{\beta^2c}+\frac{\sqrt{(x-\xi)^2-\beta^2(y-\eta)^2-\beta^2z^2}}{\beta^2c}\\ \tau_b&=\frac{(x-\xi)M}{\beta^2c}-\frac{\sqrt{(x-\xi)^2-\beta^2(y-\eta)^2-\beta^2z^2}}{\beta^2c}\end{aligned}\right\} \tag{13}$$

Functions of the time delays may then be abbreviated as

$$\left.\begin{aligned}f_a&=f(\xi,\eta,t-\tau_a)\\ f_b&=f(\xi,\eta,t-\tau_b)\\ f_{a,b}&=f(\xi,\eta,t-\tau_a)+f(\xi,\eta,t-\tau_b)\end{aligned}\right\} \tag{14}$$

In this notation, the velocity potential that is obtained by integrating the sources in the $z=0$ plane over the area S included in the forward Mach cone is

$$\varphi=-\frac{1}{2\pi}\int\int_S\frac{(w_a+w_b)d\xi\,d\eta}{\sqrt{(x-\xi)^2-\beta^2(y-\eta)^2-\beta^2z^2}}$$

$$=-\frac{1}{2\pi}\int\int_S\frac{w_{a,b}\,d\xi\,d\eta}{\sqrt{(x-\xi)^2-\beta^2(y-\eta)^2-\beta^2z^2}} \tag{15}$$

Equation (15) was derived in reference 11 for time-dependent velocity potentials and in reference 3 for time-independent velocity potentials.

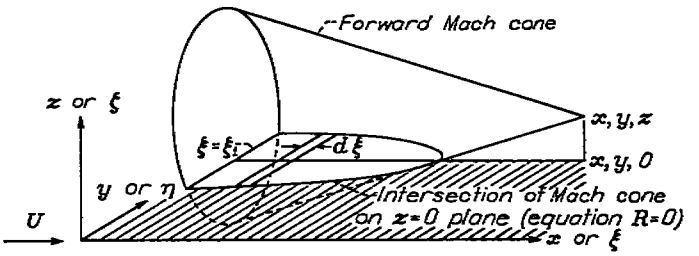

FIGURE 1.—Field of integration for evaluating velocity potential (equation (10)) near plane of sources.

A physical interpretation (reference 11) may be given for the time delays, τ_a and τ_b of equations (8), (13), and (15). If a disturbance is generated at point (ξ,η) only at time $t=0$,

the wave front from that disturbance will be spherical about a center that moves with the free-stream velocity. The trace of the waves on the $z=0$ plane is illustrated in figure 2. The wave front will enter and emerge from the point (x, y, z) at two later times τ_a and τ_b. The equation for the spherical wave path that passes through the point (x, y, z) is

$$(x-\xi-U\tau)^2+(y-\eta)^2+z^2=c^2\tau^2$$

or

$$\tau=\frac{(x-\xi)M}{\beta^2 c}\pm\frac{\sqrt{(x-\xi)^2-\beta^2(y-\eta)^2-\beta^2 z^2}}{\beta^2 c}$$

which agrees with equation (13). Thus, at a given point (x, y, z), the strength of the same wave at the two times τ_a and τ_b (in accordance with equation (15)) contributes equally to the velocity potential despite the change in the radius of the wave front. At a given time t, only the wave fronts that are entering and emerging from the point (x, y, z) contribute to the velocity potential. These two waves originated at $(\xi,\eta,0)$ at times $(t-\tau_a)$ and $(t-\tau_b)$.

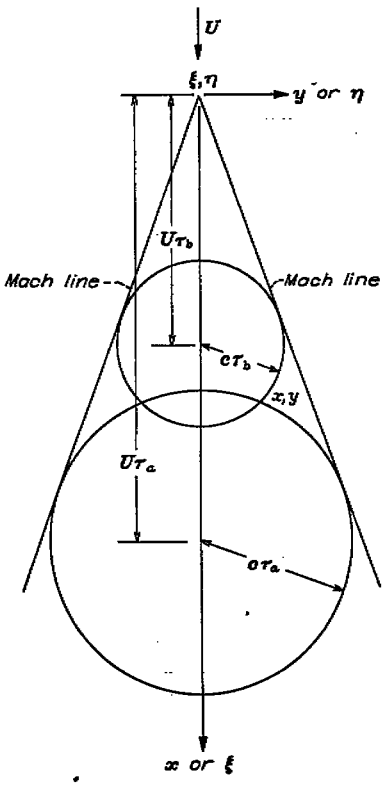

FIGURE 2.—Relation between time delays τ_a and τ_b and position of wave front.

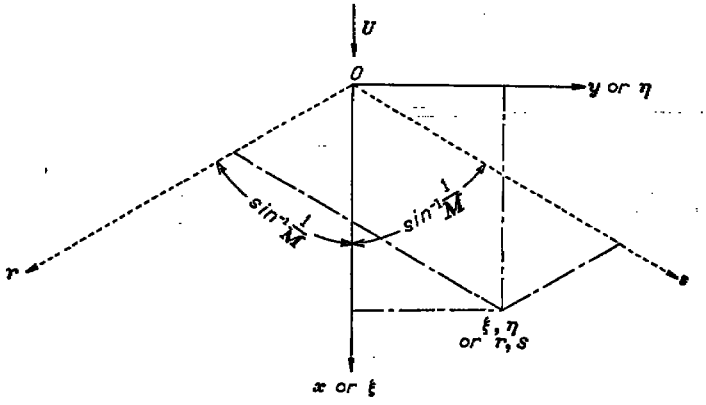

FIGURE 3.—Comparison of Cartesian and oblique coordinate systems.

The potential on the surface of the wing may be evaluated by equation (15) with z set equal to zero. The boundaries of integration then include the forward Mach lines from the point $(x,y,0)$. The integrations may generally be simplified in an oblique set of coordinates whose axes lie parallel to these Mach lines. The transformation equations relating the oblique and Cartesian coordinate systems shown in figure 3 are

$$\left.\begin{aligned} r&=\frac{M}{2\beta}(\xi-\beta\eta) & s&=\frac{M}{2\beta}(\xi+\beta\eta)\\ \xi&=\frac{\beta}{M}(s+r) & \eta&=\frac{1}{M}(s-r)\\ r_w&=\frac{M}{2\beta}(x-\beta y) & s_w&=\frac{M}{2\beta}(x+\beta y)\\ x&=\frac{\beta}{M}(s_w+r_w) & y&=\frac{1}{M}(s_w-r_w)\end{aligned}\right\} \quad (16)$$

(In references 12 to 19, the symbols u and v were employed to represent the oblique coordinates. These symbols were replaced by r and s in the present report to avoid confusion with the common usage of u and v as velocity components.)

The elemental area in the r, s coordinate system is $\frac{2\beta}{M^2}\,dr\,ds$.

Equations (15) and (13) then become (for $z=0$)

$$\varphi=-\frac{1}{2M\pi}\int\int_S\frac{w_{a,b}\,dr\,ds}{\sqrt{(r_w-r)(s_w-s)}} \quad (17)$$

$$\left.\begin{aligned}\tau_a&=\frac{M(s_w-s+r_w-r)+2\sqrt{(r_w-r)(s_w-s)}}{M\beta c}\\ \tau_b&=\frac{M(s_w-s+r_w-r)-2\sqrt{(r_w-r)(s_w-s)}}{M\beta c}\end{aligned}\right\} \quad (18)$$

If only supersonic leading edges are included in the forward Mach cone from point (r_w,s_w), w may be evaluated in terms of the effective wing slopes σ measured in η=constant planes by the relation

$$w=U\sigma \quad (19)$$

(The value of σ would thus be positive for either top or bottom surface of a wedge wing at zero angle of attack.) If a subsonic leading (or trailing) edge is also included in the forward Mach cone, the slopes of the streamlines $\lambda=\frac{w}{U}$ associated with the upwash between the wing boundary and the foremost Mach wave must be evaluated and included in the calculation (equation (17)) for the velocity potential.

Integral equation for upwash between wing boundary and foremost Mach line.—Equation (17) contains no description of the origin of w; the velocity potential in the flow field S_D of figure 4 may then be independently calculated with respect to either the top or bottom wing surfaces. These two potentials are

$$\varphi_T=-\frac{U}{2M\pi}\int\int_{S_w}\frac{(\sigma_T)_{a,b}\,dr\,ds}{\sqrt{(r_D-r)\,(s_D-s)}}-\frac{U}{2M\pi}\int\int_{S_D}\frac{\lambda_{a,b}\,dr\,ds}{\sqrt{(r_D-r)\,(s_D-s)}} \tag{20}$$

$$\varphi_B=-\frac{U}{2M\pi}\int\int_{S_w}\frac{(\sigma_B)_{a,b}\,dr\,ds}{\sqrt{(r_D-r)\,(s_D-s)}}+\frac{U}{2M\pi}\int\int_{S_D}\frac{\lambda_{a,b}\,dr\,ds}{\sqrt{(r_D-r)\,(s_D-s)}} \tag{21}$$

where r_D and s_D are the coordinates of the point at which φ is evaluated, σ_T and σ_B are the slopes of the wing on its top and bottom surfaces, and λ represents the slopes of the streamlines in the field S_D from the point of view of the top wing surface. The pressure may be calculated by substituting either equation (20) or (21) into equation (2). Because no pressure discontinuity can persist across the S_D region of the $z=0$ plane,

$$\frac{\partial\varphi_T}{\partial t}+U\frac{\partial\varphi_T}{\partial x}=\frac{\partial\varphi_B}{\partial t}+U\frac{\partial\varphi_B}{\partial x} \tag{22}$$

Equation (22) has the solution

$$\varphi_T=\varphi_B+2H(x-Ut,y) \tag{22a}$$

where H is an integration function. From equations (20), (21), and (22a), there result

$$\varphi_T=-\frac{U}{2M\pi}\int\int_{S_w}\frac{(\sigma_B+\sigma_T)_{a,b}\,dr\,ds}{2\sqrt{(r_D-r)\,(s_D-s)}}+H \tag{20a}$$

$$\varphi_B=-\frac{U}{2M\pi}\int\int_{S_w}\frac{(\sigma_B+\sigma_T)_{a,b}\,dr\,ds}{2\sqrt{(r_D-r)\,(s_D-s)}}-H \tag{21a}$$

$$-\frac{U}{2M\pi}\int\int_{S_D}\frac{\lambda_{a,b}\,dr\,ds}{\sqrt{(r_D-r)\,(s_D-s)}}=-\frac{U}{2M\pi}\int\int_{S_w}\frac{(\sigma_B-\sigma_T)_{a,b}\,dr\,ds}{2\sqrt{(r_D-r)\,(s_D-s)}}+H \tag{22b}$$

The function $2H$ represents the difference in potential across the $z=0$ plane (equation (22a)) corresponding to the strength of vorticity in the wake of the wing. For antisymmetric wings, $\sigma_B+\sigma_T=0$ and H is the potential on the top surface of the vortex sheet.

The foremost Mach wave (fig. 5) originating on the leading edge generally represents a line of infinitesimal disturbance along which H may be set equal to zero at all times. The function H remains zero along $y=$constant lines for values of x not intercepted by the wing or material body (region $S_{D,2}$ of fig. 5 (a)). The region $S_{D,1}$ generally contains a vortex sheet lying in the plane of the wing, and H is not zero. The function $H(y)$, established along the wing edge at some time t, remains unaltered for later times along a curve that sweeps downstream with the free-stream velocity and has the form of the wing trailing edge.

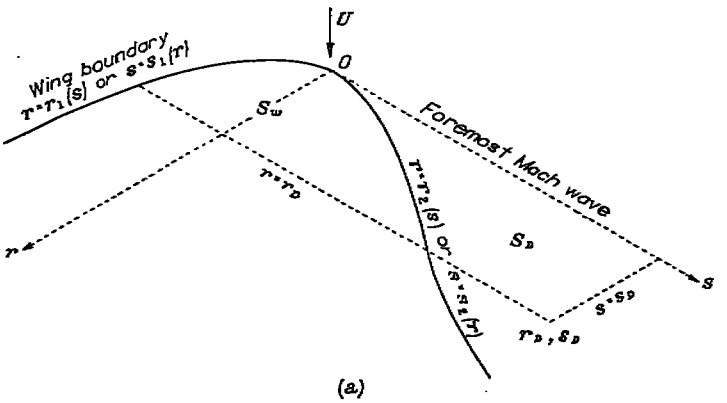

(a)

(a) Fields of integration for evaluating upwash between wing boundary and foremost Mach wave.

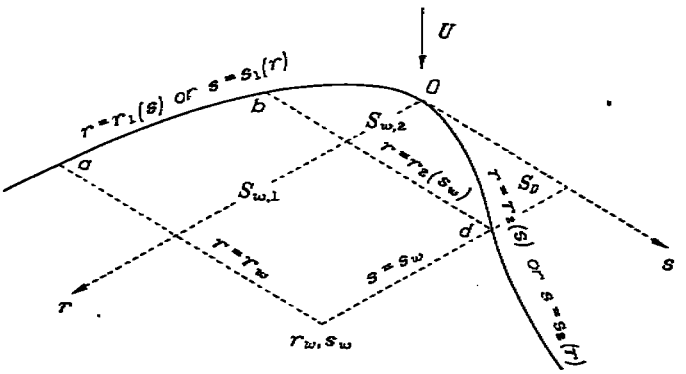

(b)

(b) Fields of integration for equations (28) and (29).

FIGURE 4.—Wing region influenced by isolated subsonic leading edge.

Equation (22b) represents the integral equation for evaluating the slopes of the streamlines in the upwash field. These slopes may generally be defined by the following two equations:

$$\int\int_{S_D}\frac{(\lambda_0)_{a,b}\,dr\,ds}{\sqrt{(r_D-r)\,(s_D-s)}}=\int\int_{S_w}\frac{(\sigma_B-\sigma_T)_{a,b}\,dr\,ds}{2\sqrt{(r_D-r)\,(s_D-s)}} \tag{23}$$

and

$$\int\int_{S_D}\frac{(\lambda_H)_{a,b}\,dr\,ds}{\sqrt{(r_D-r)\,(s_D-s)}}=-\frac{2M\pi}{U}H \tag{24}$$

The actual slope λ is then the sum of the solutions for the slopes obtained from equations (23) and (24):

$$\lambda=\lambda_0+\lambda_H \qquad (25)$$

For regions such as S_D of figure 4 (a), $H=0$ and only equation (23) need be considered. For steady-state solutions, the time-delay notation a, b may be disregarded in equation (23).

II—TIME-INDEPENDENT FLOWS

The concept leading to the derivation of equations (23) and (24) may be extended in principle to define the upwash velocity components in the plane of arbitrary thin wings at supersonic speeds. Equation (17) then yields the velocity potential from which the aerodynamic coefficients may be derived. The effects of the upwash field have been evaluated for a class of curved plan-form wings, and the corresponding velocity potentials of time-independent configurations have been derived. Included in the calculations are wings with subsonic leading and trailing edges connected to supersonic leading edges and a few cases of wing regions influenced by interacting upwash fields.

Evaluation of isolated regions of upwash off subsonic leading edges.—The steady-state solution of equation (23) is conveniently derived for the wing of figure 4. The origin of coordinates is placed at the junction of the supersonic and subsonic leading edges. These are defined, respectively, by the equations

$$\left.\begin{aligned} s=s_1(r) \quad &\text{or} \quad r=r_1(s) \\ s=s_2(r) \quad &\text{or} \quad r=r_2(s) \end{aligned}\right\} \qquad (26)$$

Equation (23) then becomes

$$\int_0^{r_D}\frac{dr}{\sqrt{r_D-r}}\int_{s_2(r)}^{s_D}\frac{\lambda\,ds}{\sqrt{s_D-s}}=\int_0^{r_D}\frac{dr}{\sqrt{r_D-r}}\int_{s_1(r)}^{s_2(r)}\frac{(\sigma_B-\sigma_T)ds}{2\sqrt{s_D-s}} \qquad (27)$$

(Inasmuch as λ_H is zero, λ_0 is replaced by λ in equation (27).)

Because equation (27) must hold for all values of r_D, which does not appear in the integration with respect to s, the equation may be reduced to

$$\int_{s_2(r)}^{s_D}\frac{\lambda\,ds}{\sqrt{s_D-s}}=\int_{s_1(r)}^{s_2(r)}\frac{(\sigma_B-\sigma_T)ds}{2\sqrt{s_D-s}} \qquad (27a)$$

This reduction shows that for steady-state solutions only the wing slopes along the forward Mach line contribute to the upwash at the point (r_D, s_D).

Equation (27a) may be solved, as in reference 14, as an example of Abel's equation (references 20 and 21) to give

$$\lambda(r,s)=\frac{1}{\pi}\frac{\partial}{\partial s}\int_{s_2(r)}^{s}\frac{ds_D}{\sqrt{s-s_D}}\int_{s_1(r)}^{s_2(r)}\frac{(\sigma_B-\sigma_T)dv}{2\sqrt{s_D-v}} \qquad (27b)$$

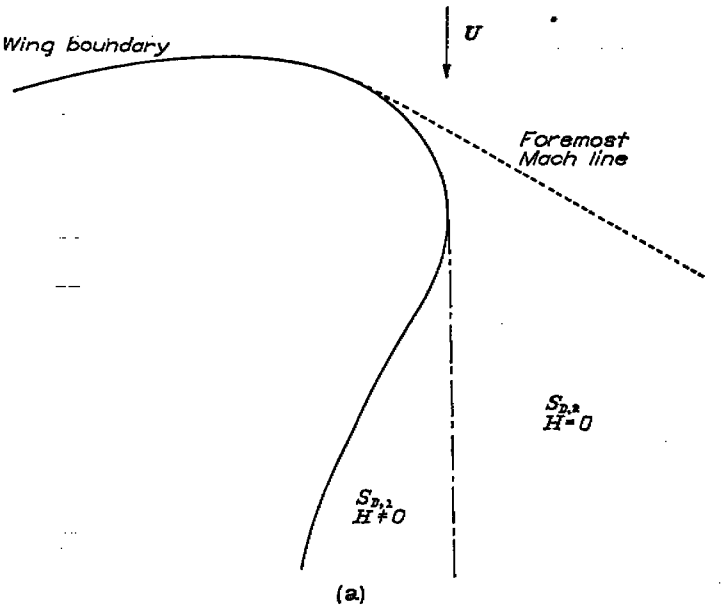

(a)

(a) Division of external field S_D for evaluation of H.

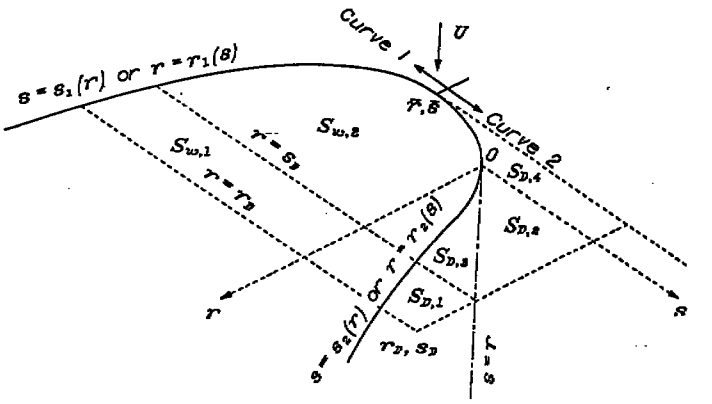

(b)

(b) Point (r_D, s_D) on vortex sheet.

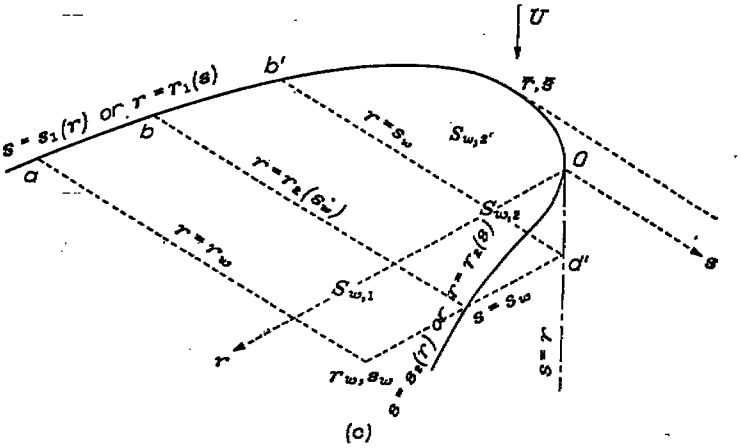

(c)

(c) Point (r_w, s_w) on wing surface.

FIGURE 5.—Integration boundaries for evaluating wing region influenced by subsonic trailing edge.

where v has replaced s as a variable of integration. Equation (27b) may also be expressed in differential form as

$$\frac{d\lambda}{dv}=\frac{(\sigma_B-\sigma_T)\sqrt{s_2-v}}{2\pi(s-v)\sqrt{s-s_2}} \tag{27c}$$

where a wing element of length dv and having the effective slope $\frac{\sigma_B-\sigma_T}{2}$ at point (r,v) produces an increment $d\lambda$ at point (r,s) (fig. 6). Either by interchange of the order of integration in equation (27b) or by integration of equation (27c), an alternative expression for λ results

$$\lambda(r,s)=\frac{1}{2\pi\sqrt{s-s_2}}\int_{s_1}^{s_2}\frac{(\sigma_B-\sigma_T)\sqrt{s_2-v}\,dv}{s-v} \tag{27d}$$

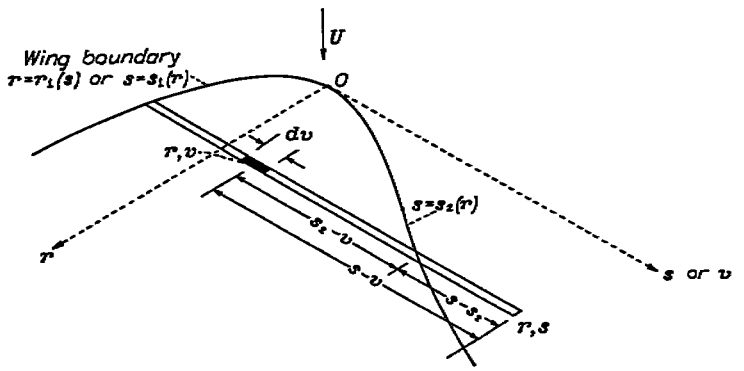

FIGURE 6.—Geometric significance of factors in equation (27d).

If $(\sigma_B-\sigma_T)$ is independent of s, either equation (27b) or (27d) gives

$$\lambda(r,s)=\frac{(\sigma_B-\sigma_T)}{\pi}\left[\sqrt{\frac{s_2(r)-s_1(r)}{s-s_2(r)}}-\tan^{-1}\sqrt{\frac{s_2(r)-s_1(r)}{s-s_2(r)}}\right] \tag{27e}$$

Aerodynamic effects of isolated regions of upwash.—The contribution φ_D of the upwash field S_D to the velocity potential on the surface of the wing in figure 4(b) may be computed from equations (17) and (19) as

$$\varphi_D=-\frac{U}{M\pi}\int_0^{r_2(s_w)}\frac{dr}{\sqrt{r_w-r}}\int_{s_2(r)}^{s_w}\frac{\lambda\,ds}{\sqrt{s_w-s}} \tag{28}$$

If λ is eliminated from equation (28) by means of either equation (27a) or equation (27d), there results

$$\varphi_D=-\frac{U}{M\pi}\int_0^{r_2(s_w)}\frac{dr}{\sqrt{r_w-r}}\int_{s_1(r)}^{s_2(r)}\frac{(\sigma_B-\sigma_T)}{2}\frac{ds}{\sqrt{s_w-s}}$$

$$=-\frac{U}{M\pi}\int\int_{S_{w,2}}\frac{(\sigma_B-\sigma_T)}{2}\frac{dr\,ds}{\sqrt{(r_w-r)(s_w-s)}} \tag{28a}$$

The contribution of the upwash field is thus replaced by an equivalent contribution on the wing surface. The surface velocity potential at (r_w, s_w) then becomes

$$\varphi=-\frac{U}{M\pi}\int\int_{S_{w,1}}\frac{\sigma_T\,dr\,ds}{\sqrt{(r_w-r)(s_w-s)}}-\frac{U}{M\pi}\int\int_{S_{w,2}}\frac{(\sigma_B+\sigma_T)}{2}\frac{dr\,ds}{\sqrt{(r_w-r)(s_w-s)}} \tag{29}$$

For thin-plate wings, or for antisymmetric solutions (such as evaluation of the effect of uniform rate of roll), $(\sigma_B+\sigma_T)=0$ so that the integration over the area $S_{w,2}$ vanishes. In this case, the contribution to φ of the upwash field cancels the direct contribution of the part of the wing that generated the upwash field. Hence, alteration of the thin-plate-wing plan boundaries in the region $S_{w,2}$ (fig. 4 (b)) does not alter the surface velocity potential at point (r_w,s_w). (An elegant derivation of this fact is presented in reference 22. Because there is no contribution to the velocity potential ahead of the forward Mach cone, equation (17) may be written for steady boundary conditions as

$$\varphi=-\frac{1}{M\pi}\int_{-\infty}^{r_w}\int_{-\infty}^{s_w}\frac{w\,dr\,ds}{\sqrt{(r_w-r)(s_w-s)}}$$

Two auxiliary point functions may now be defined as

$$X(r_w,s)=-\frac{1}{M\pi}\int_{-\infty}^{r_w}\frac{w\,dr}{\sqrt{r_w-r}}$$

$$Y(r,s_w)=-\frac{1}{M\pi}\int_{-\infty}^{s_w}\frac{w\,ds}{\sqrt{s_w-s}}$$

In terms of these point functions, the velocity potential is

$$\varphi=\int_{-\infty}^{s_w}\frac{X\,ds}{\sqrt{s_w-s}}\text{ or }\varphi=\int_{-\infty}^{r_w}\frac{Y\,dr}{\sqrt{r_w-r}}$$

Each of these equations for X, Y, and φ are forms of Abel's equation and may be solved accordingly. For an antisymmetric wing of plan boundary as shown on fig. 4 (b), $\varphi\,(r,s_w)=0$ if $r<r_2(s_w)$. Hence Y is zero for this range also. The velocity potential may then be evaluated only from the region $S_{w,1}$ of fig. 4 (b).) Pressure coefficients may be obtained by substituting φ from equation (29) into equation (2a). Perturbation-velocity components are obtained from the gradient of φ.

As illustrations of equation (29), two examples are presented. The first is a wedge wing (fig. 7) with plan-boundary equations $s=-k_1r$ and $s=k_2r$. The wing slopes are taken as $\sigma_B=\sigma+\alpha$ and $\sigma_T=\sigma-\alpha$, where 2σ is the wedge angle and α is the angle of attack. The velocity potential on the top surface of the wing is then (reference 12)

$$\varphi=-\frac{2U\sigma}{M\pi}\left[\frac{s_w+k_1r_w}{\sqrt{k_1}}\tan^{-1}\sqrt{\frac{k_1r_w}{s_w}}+\frac{(s_w-k_2r_w)}{\sqrt{k_2}}\times\log_e\frac{\sqrt{k_2r_w-s_w}}{\sqrt{k_2r_w}+\sqrt{s_w}}\right]+\frac{2U\alpha}{M\pi}\left[\sqrt{\frac{k_1+k_2}{k_2^2}s_w(k_2r_w-s_w)}+\frac{(s_w+k_1r_w)}{\sqrt{k_1}}\tan^{-1}\sqrt{\frac{k_1(k_2r_w-s_w)}{(k_1+k_2)s_w}}\right] \tag{30}$$

This solution for φ is the addition of terms that are dependent on and independent of the angle of attack. The effects of angle of attack may therefore be evaluated on flat-plate wings whose plan boundaries coincide with those of the chosen wing. This example illustrates a general superposition principle that follows directly from the linearity of equation (15) with respect to either w or σ (from equation (19)).

The velocity potential of a flat-plate wing (fig. 8) having a straight-line leading edge $s=-k_1 r$ coupled to an arbitrary subsonic leading edge $s=s_2(r)$ or $r=r_2(s)$ may also be evaluated explicitly. In this example, $\sigma_B=-\sigma_T=\alpha$, so that φ is

$$\varphi=\frac{2U\alpha}{M\pi}\left[\sqrt{(s_w+k_1r_2)(r_w-r_2)}+\frac{k_1r_w+s_w}{\sqrt{k_1}}\tan^{-1}\sqrt{\frac{k_1(r_w-r_2)}{(s_w+k_1r_2)}}\right] \quad (31)$$

where r_2 is a function of s_w. The factor multiplying α in equation (30) may also be obtained from equation (31) by setting $r_2=\frac{s_w}{k_2}$.

Some complications occur if the supersonic leading edge is connected to two subsonic leading edges that are located in the forward Mach cone from the point (r_w, s_w) (fig. 9). The contributions to the velocity potential of each of the upwash fields may be independently calculated from equations (28) and (28a) to give

$$-\frac{U}{M\pi}\int\int_{S_{D,1}}\frac{\lambda_1\,dr\,ds}{\sqrt{(r_w-r)(s_w-s)}}=-\frac{U}{M\pi}\int\int_{S_{w(1+2)}}\frac{(\sigma_B-\sigma_T)\,dr\,ds}{2\sqrt{(r_w-r)(s_w-s)}} \quad (32)$$

$$-\frac{U}{M\pi}\int\int_{S_{D,2}}\frac{\lambda_2\,dr\,ds}{\sqrt{(r_w-r)(s_w-s)}}=-\frac{U}{M\pi}\int\int_{S_{w(3+3)}}\frac{(\sigma_B-\sigma_T)\,dr\,ds}{2\sqrt{(r_w-r)(s_w-s)}} \quad (33)$$

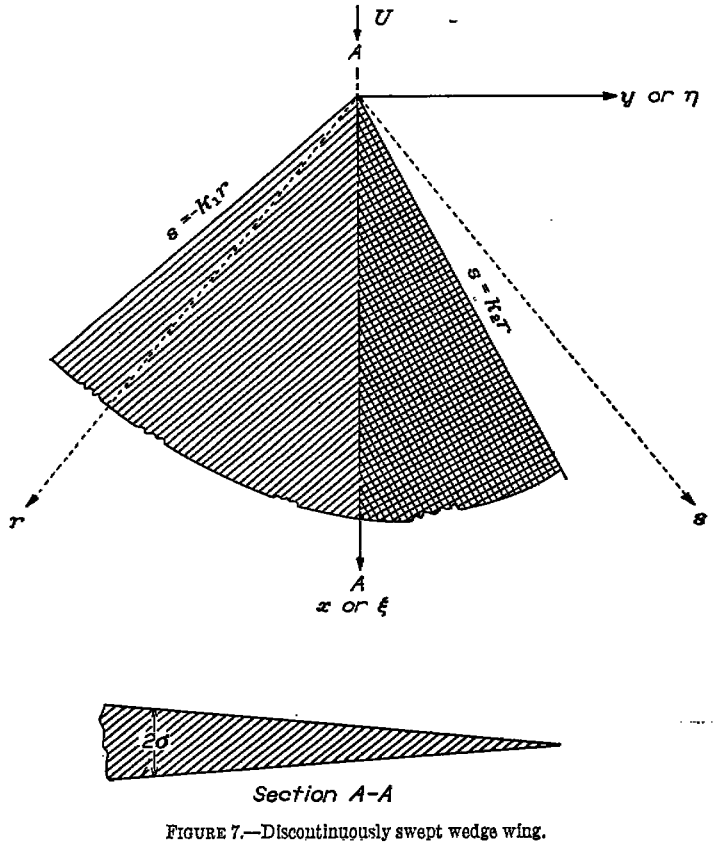

FIGURE 7.—Discontinuously swept wedge wing.

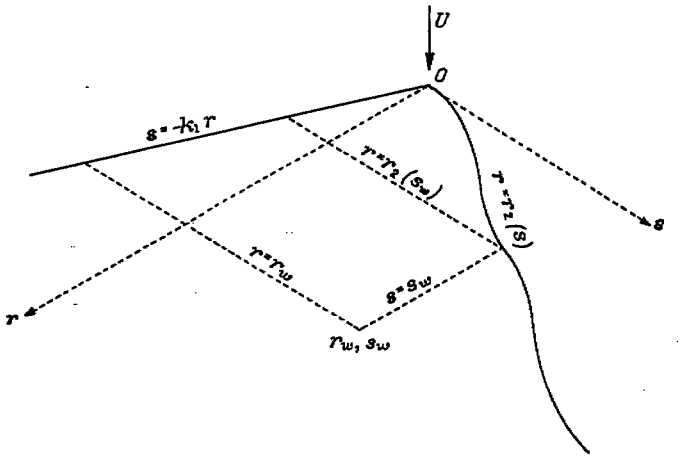

FIGURE 8.—Boundary limits for equation (31).

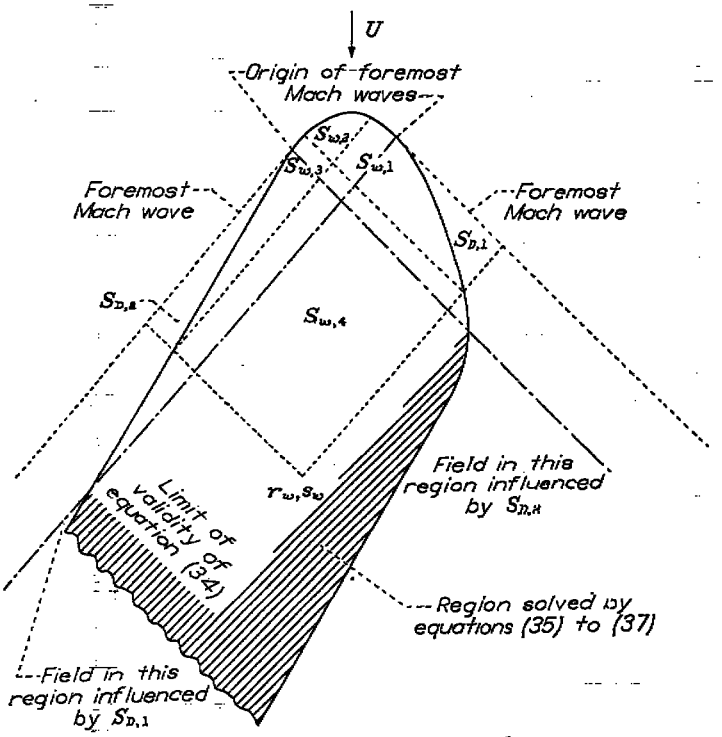

FIGURE 9.—Regions of integration for calculating velocity potential on surface of wing of finite thickness influenced by two independent perturbed flow fields external to wing surface.

Addition of these contributions to those of the wing area $S_{w(1+2+3+4)}$, as evaluated by equations (17) and (19), gives (reference 12)

$$\varphi=-\frac{U}{M\pi}\int\int_{S_{w(1+3)}}\frac{(\sigma_B+\sigma_T)\,dr\,ds}{2\sqrt{(r_w-r)(s_w-s)}}-\frac{U}{M\pi}\int\int_{S_{w,2}}\frac{\sigma_B\,dr\,ds}{\sqrt{(r_w-r)(s_w-s)}}-\frac{U}{M\pi}\int\int_{S_{w,4}}\frac{\sigma_T\,dr\,ds}{\sqrt{(r_w-r)(s_w-s)}} \quad (34)$$

The role of σ_T and σ_B is thus effectively interchanged for the regions of integration $S_{w,2}$. Likewise, for antisymmetric configurations ($\sigma_B+\sigma_T=0$), the areas $S_{w,1}$ and $S_{w,3}$ give no contribution to the velocity potential.

Aerodynamic effects of interacting regions of upwash.—If interacting upwash fields are included in the forward Mach cone from the point (r_w, s_w), as in the shaded region of figure 9, parts of the upwash field must be evaluated before the velocity potential can be computed. The effective wing in application of equation (34) includes the upwash fields $S_{D,1}$ and $S_{D,2}$ (fig. 10) for which $\sigma_B = -\lambda$. The velocity potential may then be written

$$\varphi = -\frac{U}{M\pi}\int\int_{S_{w(1+3)}} \frac{(\sigma_B+\sigma_T)\,dr\,ds}{2\sqrt{(r_w-r)(s_w-s)}} - \frac{U}{M\pi}\int\int_{S_{w,2}} \frac{\sigma_B\,dr\,ds}{\sqrt{(r_w-r)(s_w-s)}} - \frac{U}{M\pi}\int\int_{S_{w,4}} \frac{\sigma_T\,dr\,ds}{\sqrt{(r_w-r)(s_w-s)}} + \frac{U}{M\pi}\int\int_{S_{D,1}} \frac{\lambda_1\,dr\,ds}{\sqrt{(r_w-r)(s_w-s)}} + \frac{U}{M\pi}\int\int_{S_{D,2}} \frac{\lambda_2\,dr\,ds}{\sqrt{(r_w-r)(s_w-s)}} \tag{35}$$

Each of the upwash streamline slopes may be evaluated by equations similar to equation (27d). In the notation of figure 10 (and with v replacing s as a variable of integration), the contribution of the flow field $S_{D,1}$ is

$$-\frac{U}{M\pi}\int\int_{S_D} \frac{\lambda_1\,dr\,dv}{\sqrt{(r_w-r)(s_w-v)}} = -\frac{U}{M\pi}\int_0^{r_2(s_3)} \frac{dr}{\sqrt{r_w-r}}\int_{s_1(r_w)}^{s_2(r_w)} \frac{\lambda(r,v)\,dv}{\sqrt{s_w-v}}$$

$$= -\frac{U}{2M\pi^2}\int_0^{r_2(s_3)} \frac{dr}{\sqrt{(r_w-r)}}\int_{s_1(r)}^{s_2(r_w)} \frac{dv}{\sqrt{(s_w-v)(v-s_2)}}\int_{s_1(r)}^{s_2(r)} \frac{(\sigma_B-\sigma_T)\sqrt{s_2-s}\,ds}{(v-s)} \tag{36}$$

Interchange of the order of integration with respect to v and s and evaluation of the integral with respect to v give

$$-\frac{U}{M\pi}\int\int_{S_{D,1}} \frac{\lambda_1\,dr\,ds}{\sqrt{(r_w-r)(s_w-s)}} = -\frac{U}{2M\pi^2}\int\int_{S_{w,2}} \left[\frac{\pi}{2}+\tan^{-1}\frac{(s_3-s)(s_w+s_2-2s)-2(s_2-s)(s_w-s)}{2\sqrt{(s_2-s)(s_w-s)(s_w-s_3)(s_3-s_2)}}\right] \frac{(\sigma_B-\sigma_T)\,dr\,ds}{\sqrt{(r_w-r)(s_w-s)}} \tag{36a}$$

where s_3 is a function of r_w and s_2 is a function of r. (Equation (36a) reduces to the form of equation (28) when $s_w = s_3(r_w)$.) Likewise,

$$-\frac{U}{M\pi}\int\int_{S_{D,2}} \frac{\lambda_2\,dr\,ds}{\sqrt{(r_w-r)(s_w-s)}} = -\frac{U}{2M\pi^2}\int\int_{S_{w,3}} \left[\frac{\pi}{2}+\tan^{-1}\frac{(r_2-r)(r_w+r_3-2r)-2(r_3-r)(r_w-r)}{2\sqrt{(r_3-r)(r_w-r)(r_w-r_2)(r_2-r_3)}}\right] \frac{(\sigma_B-\sigma_T)\,dr\,ds}{\sqrt{(r_w-r)(s_w-s)}} \tag{37}$$

where r_2 is a function of s_w and r_3 is a function of s. Elimination of λ_1 and λ_2 between equations (35), (36a), and (37) yields the velocity potential in terms of the wing slopes and plan-boundary equations. An alternative scheme (suggested in reference 14) would be to derive all of the upwash slopes λ by means of equations similar to equations (27b) or (27d) and then to evaluate φ directly from equations (17) and (19). More complicated examples including doubly interacting external upwash fields may be solved in a similar manner.

If the upwash fields continuously interact as they do for the wing shown in figure 11, the solution of an integral equation is required (reference 14). The slopes of the streamlines from equation (27d) in the upwash region $S_{D,1}$ are

$$\lambda_1(r,s) = \frac{1}{\pi\sqrt{s-s_2}}\left[\int_{s_1}^{s_2} \frac{(\sigma_B-\sigma_T)\sqrt{s_2-v}}{2(s-v)}\,dv - \int_0^{s_2} \frac{\lambda_2(r,v)\sqrt{s_2-v}}{(s-v)}\,dv\right] \tag{38}$$

where v is the integration variable in the s direction and s_2 and s_3 are functions of r.

Similarly,

$$\lambda_2(r,s) = \frac{1}{\pi\sqrt{r-r_3}}\left[\int_{r_2}^{r_3} \frac{(\sigma_B-\sigma_T)\sqrt{r_3-u}}{2(r-u)}\,du - \int_0^{r_2} \frac{\lambda_1(u,s)\sqrt{r_3-u}}{(r-u)}\,du\right] \tag{39}$$

where u is the integration variable in the r direction and r_2 and r_3 are functions of s. The functions λ_1 and λ_2 can there-

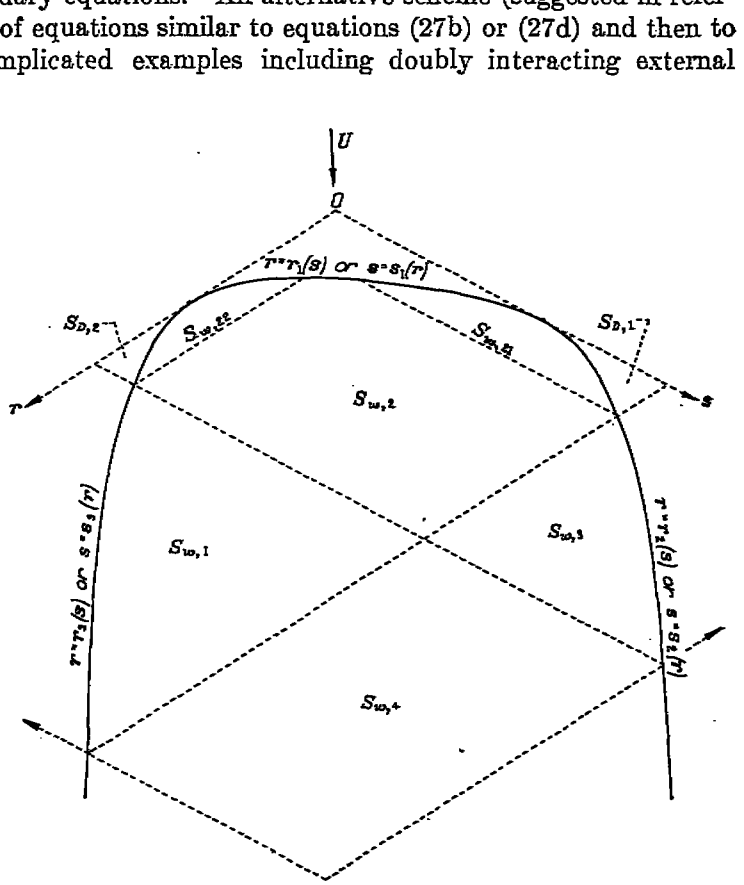

FIGURE 10.—Wing including regions of interacting upwash fields.

fore be determined from the two equations, at least in principle, either by successive approximations or by direct substitution and solution of the resulting integral equation. (If the wing has a symmetrical plan form about the x-axis, $\lambda_2(r,s)=\lambda_1(s,r)$ and the two equations (35) and (36) become the same. If the flow is conical, either λ_1 or λ_2 is a function of s/r.) Once the slopes of the streamlines in the upwash field are determined, the velocity potential may be evaluated from equations (17) and (19).

Calculation of perturbation-velocity components.—The perturbation-velocity components may be obtained by partial differentiation of the velocity potential. This differentiation may be performed prior to the integrations indicated in equations such as (17), (29), (34), and so forth. The method is illustrated, as in reference 15, for the wing of figure 12, which includes only supersonic leading edges in the forward Mach cone. If the velocity potential is computed at point (x,y) and at point $(x+dx,y)$, the result is

$$\varphi=-\frac{U}{\pi}\int\int_S \frac{\sigma\, d\xi\, d\eta}{\sqrt{(x-\xi)^2-\beta^2(y-\eta)^2}} \tag{40}$$

$$\varphi+\frac{\partial\varphi}{\partial x}dx=-\frac{U}{\pi}\int\int_S \frac{\left(\sigma+\frac{\partial\sigma}{\partial\xi}dx\right)d\xi\, d\eta}{\sqrt{(x-\xi)^2-\beta^2(y-\eta)^2}}-\frac{U}{\pi}dx\int_{\text{abd}}\frac{\sigma\, d\eta}{\sqrt{(x-\xi)^2-\beta^2(y-\eta)^2}} \tag{41}$$

where the line integral is evaluated along the line abd, and the coordinate ξ may be eliminated from the line integral by means of the equation for the leading edge. Subtraction of equation (40) from equation (41) and cancellation of dx yield

$$\frac{\partial\varphi}{\partial x}=-\frac{U}{\pi}\int\int_S \frac{\frac{\partial\sigma}{\partial\xi}d\xi\, d\eta}{\sqrt{(x-\xi)^2-\beta^2(y-\eta)^2}}-\frac{U}{\pi}\int_{\text{abd}}\frac{\sigma\, d\eta}{\sqrt{(x-\xi)^2-\beta^2(y-\eta)^2}} \tag{42}$$

This result may also be obtained by formal differentiation of equation (40). In a similar manner

$$\frac{\partial\varphi}{\partial y}=-\frac{U}{\pi}\int\int_S \frac{\frac{\partial\sigma}{\partial\eta}d\xi\, d\eta}{\sqrt{(x-\xi)^2-\beta^2(y-\eta)^2}}+\frac{U}{\pi}\int_{\text{abd}}\frac{\sigma\, d\xi}{\sqrt{(x-\xi)^2-\beta^2(y-\eta)^2}} \tag{43}$$

Equations (42) and (43) may also be written in the oblique coordinates as

$$\frac{\partial\varphi}{\partial x}=-\frac{U}{2\beta\pi}\int\int_S \frac{\left(\frac{\partial\sigma}{\partial r}+\frac{\partial\sigma}{\partial s}\right)dr\, ds}{\sqrt{(r_w-r)(s_w-s)}}-\frac{U}{2\beta\pi}\int_{\text{abd}}\frac{\sigma(ds-dr)}{\sqrt{(r_w-r)(s_w-s)}} \tag{42a}$$

$$\frac{\partial\varphi}{\partial y}=-\frac{U}{2\pi}\int\int_S \frac{\left(\frac{\partial\sigma}{\partial s}-\frac{\partial\sigma}{\partial r}\right)dr\, ds}{\sqrt{(r_w-r)(s_w-s)}}+\frac{U}{2\pi}\int_{\text{abd}}\frac{\sigma(ds+dr)}{\sqrt{(r_w-r)(s_w-s)}} \tag{43a}$$

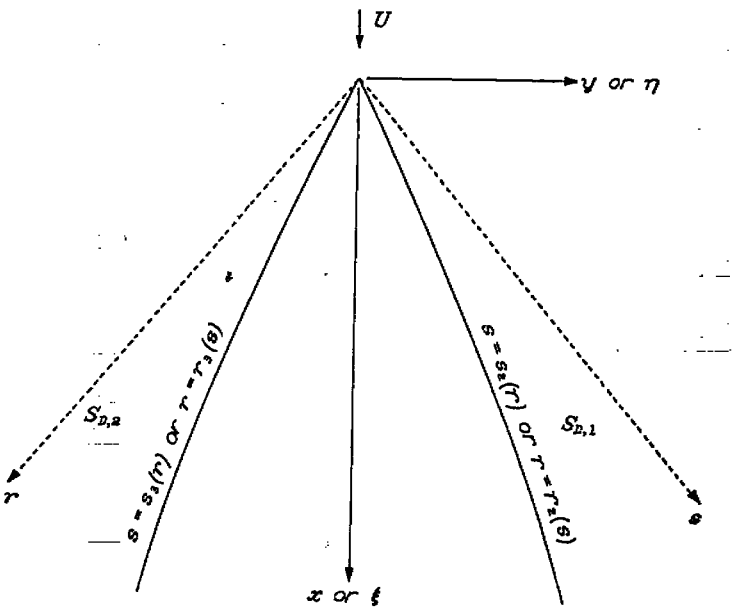

FIGURE 11.—Wing plan form and areas of upwash for equations (38) and (39).

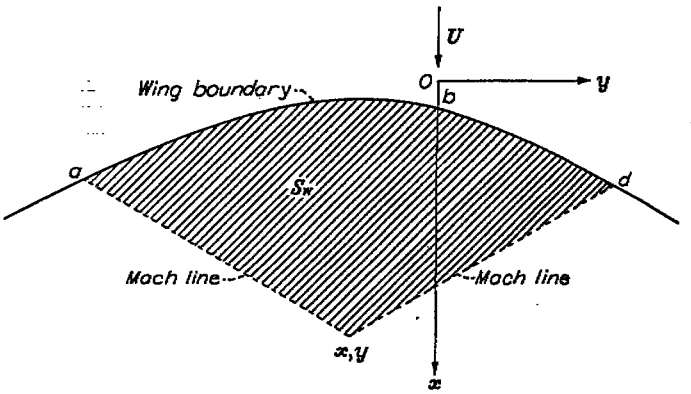

(a)

(a) Wing point (x, y).

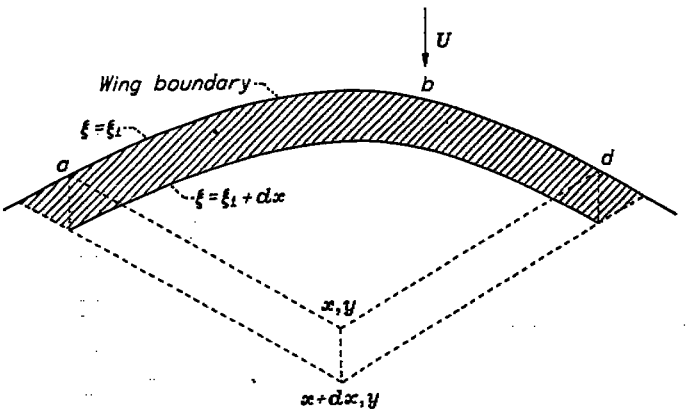

(b)

(b) Wing point $(x+dx, y)$.

FIGURE 12.—Fields of integration for equations (40) to (42).

The line integral of equation (42) corresponds to the discontinuous change in flow direction that occurs along the leading edge, and the surface integral corresponds to continuous changes in slopes over the wing plan area. (Evaluation of the surface integral along lines of discontinuous $\frac{\partial \sigma}{\partial \xi}$ results in additional line integrals.) The impulses that lead to the pressure distributions on supersonic wings are thus generated at points where the flow direction is altered. For flat surface wings, these impulses are generated only along the leading edge.

When the surface velocity potential is influenced by an upwash field, as in figure 4, the velocity potential may be calculated from equation (29). The evaluation of the perturbation-velocity components is similar to the derivations of equations (42) and (43) except that there is effectively a shifting line of discontinuous wing slopes between the plan areas $S_{w,1}$ and $S_{w,2}$, which adds line integrals to the calculation (reference 15). The partial differentiations of φ with respect to x and y (fig. 4 (b)) have been evaluated in appendix B and are expressed in oblique coordinates as

$$\frac{\partial \varphi}{\partial x}=-\frac{U}{2\beta\pi}\int\int_{S_{w,1}}\frac{\left(\frac{\partial \sigma_T}{\partial r}+\frac{\partial \sigma_T}{\partial s}\right)dr\,ds}{\sqrt{(r_w-r)(s_w-s)}}-\frac{U}{4\beta\pi}\int\int_{S_{w,2}}\frac{\left[\frac{\partial(\sigma_B+\sigma_T)}{\partial r}+\frac{\partial(\sigma_B+\sigma_T)}{\partial s}\right]dr\,ds}{\sqrt{(r_w-r)(s_w-s)}}-\frac{U}{2\beta\pi}\int_{ab}\frac{\sigma_T(ds-dr)}{\sqrt{(r_w-r)(s_w-s)}}-$$

$$\frac{U}{4\beta\pi}\int_{b0d}\frac{(\sigma_B+\sigma_T)(ds-dr)}{\sqrt{(r_w-r)(s_w-s)}}-\frac{U}{4\beta\pi}\frac{\left(1-\frac{dr_2}{ds_w}\right)}{\sqrt{r_w-r_2}}\int_{bd}\frac{(\sigma_T-\sigma_B)ds}{\sqrt{s_w-s}} \tag{44}$$

$$\frac{\partial \varphi}{\partial y}=-\frac{U}{2\pi}\int\int_{S_{w,1}}\frac{\left(\frac{\partial \sigma_T}{\partial s}-\frac{\partial \sigma_T}{\partial r}\right)dr\,ds}{\sqrt{(r_w-r)(s_w-s)}}-\frac{U}{4\pi}\int\int_{S_{w,2}}\frac{\left[\frac{\partial(\sigma_B+\sigma_T)}{\partial s}-\frac{\partial(\sigma_B+\sigma_T)}{\partial r}\right]dr\,ds}{\sqrt{(r_w-r)(s_w-s)}}+\frac{U}{2\pi}\int_{ab}\frac{\sigma_T(ds+dr)}{\sqrt{(r_w-r)(s_w-s)}}+$$

$$\frac{U}{2\pi}\int_{b0d}\frac{(\sigma_B+\sigma_T)}{2}\frac{(ds+dr)}{\sqrt{(r_w-r)(s_w-s)}}+\frac{U}{4\pi}\frac{\left(1+\frac{dr_2}{ds_w}\right)}{\sqrt{r_w-r_2}}\int_{bd}\frac{(\sigma_T-\sigma_B)ds}{\sqrt{s_w-s}} \tag{45}$$

where r_2 is the wing-plan-boundary equation $r=r_2(s_w)$. The more complicated expressions, such as equation (34) and combinations of equations (35), (36), and (37), can be treated in a similar manner.

The expressions for the perturbation-velocity components are simplified for flat-plate wings having slopes $\sigma_B=-\sigma_T=\alpha$. (These components may also be regarded as the contribution associated with angle of attack on a cambered wing.) Equations (44) and (45) may then be written

$$\frac{\partial \varphi}{\partial x}=\frac{U\alpha}{2\beta\pi}\int_{ab}\frac{(ds-dr)}{\sqrt{(r_w-r)(s_w-s)}}+\frac{U\alpha}{\beta\pi}\left(1-\frac{dr_2}{ds_w}\right)\sqrt{\frac{s_w-s_1(r_2)}{r_w-r_2}} \tag{46}$$

and

$$\frac{\partial \varphi}{\partial y}=-\frac{U\alpha}{2\pi}\int_{ab}\frac{(ds+dr)}{\sqrt{(r_w-r)(s_w-s)}}-\frac{U\alpha}{\pi}\left(1+\frac{dr_2}{ds_w}\right)\sqrt{\frac{s_w-s_1(r_2)}{r_w-r_2}} \tag{47}$$

The line integrals of equations (46) and (47) may be numerically or graphically evaluated by the procedures outlined in reference 16. If the supersonic leading edge conforms to the equation $s=-k_1r$, equations (46) and (47) give

$$\frac{\partial \varphi}{\partial x}=\frac{U\alpha}{\beta\pi}\left[\left(1-\frac{dr_2}{ds_w}\right)\sqrt{\frac{s_w+k_1r_2}{r_w-r_2}}+\frac{(k_1+1)}{\sqrt{k_1}}\tan^{-1}\sqrt{\frac{k_1(r_w-r_2)}{s_w+k_1r_2}}\right] \tag{48}$$

$$\frac{\partial \varphi}{\partial y}=-\frac{U\alpha}{\pi}\left[\left(1+\frac{dr_2}{ds_w}\right)\sqrt{\frac{s_w+k_1r_2}{r_w-r_2}}+\frac{(k_1-1)}{\sqrt{k_1}}\tan^{-1}\sqrt{\frac{k_1(r_w-r_2)}{s_w+k_1r_2}}\right] \tag{49}$$

Equations (48) and (49) could also be obtained by partial differentiation of equation (31).

Along the subsonic leading edge, $(r_w-r_2)=0$ and an infinity occurs in the perturbation-velocity component of equations (46) and (47). This infinity represents a breakdown in the validity of the linearized theory, and corresponds to the formation of a stagnation point near the leading edge of two-dimensional subsonic airfoils. Even though unbounded pressures may be obtained from equations (2a) and (46), these values should be interpreted as representing some fraction of free-stream stagnation pressure (or near-vacuum conditions). As was observed in reference 23, discontinuities in wing-plan-boundary tangents along subsonic leading edges lead to discontinuities in the x and y pertubation-velocity components and in the wing loading along the Mach line from the discontinuity.

A physical consideration of pressure disturbances from the wing-plan boundaries indicates that the velocity component lying parallel to the edge must be continuous across the wing edge. This concept is evident from oblique-shock relations for supersonic leading and trailing edges and may be verified by equations (20), (46), and (47) for a class of subsonic leading edges. All changes in the velocity at the wing-plan boundary must therefore occur in the velocity component perpendicular to the edge.

Evaluation of suction forces on subsonic leading edges.—Near the wing edge, the line integrals of equations (46) and (47) are zero. Likewise, the direction slope of the perturbation velocity is

$$\frac{\frac{\partial \varphi}{\partial y}}{\frac{\partial \varphi}{\partial x}}=\frac{-\beta\left(1+\frac{dr_2}{ds_w}\right)}{\left(1-\frac{dr_2}{ds_w}\right)}=-\left(\frac{dx}{dy}\right)_2 \tag{50}$$

where $\left(\frac{dx}{dy}\right)_2$ is evaluated from the wing-plan-boundary equation. The perturbation velocity is thus normal to the wing-tip boundary and has the value

$$\lim_{\substack{n\to 0\\ s_w\to s_2\\ r_w\to r_2}}\frac{\partial \varphi}{\partial n}=\pm\frac{U\alpha}{\beta\pi}\sqrt{\left(\frac{s_w-s_1}{r_w-r_2}\right)\left[\left(1-\frac{dr_2}{ds_w}\right)^2+\beta^2\left(1+\frac{dr_2}{ds_w}\right)^2\right]} \tag{51}$$

In accordance with references 24, 7, and 19, this type of variation in $\frac{\partial \varphi}{\partial n}$ as $n \to 0$ leads to a suction force per unit length along the leading edge of magnitude

$$\lim_{s_w \to s_2} \frac{dF_n}{dl} = \frac{4\rho U^2 \alpha^2 (s_w - s_1)}{\pi M} \sqrt{\frac{dr_2}{ds_w}} \tag{52}$$

where F_n is the force normal to the leading edge and dl is an infinitesimal distance along that edge. If dl is expressed in terms of ds and F is defined as the suction force in the flight direction, equation (52) may alternatively be written

$$\lim_{s_w \to s_2} \frac{dF}{ds} = \frac{4\rho U^2 \alpha^2 (s_w - s_1)}{\pi M^2} \left(1 - \frac{dr_2}{ds_w}\right) \sqrt{\frac{dr_2}{ds_w}} \tag{53}$$

The suction force along subsonic leading edges can thus be evaluated explicitly by equation (53) for wing boundaries that are not influenced by interacting upwash flow fields. Equation (53) has been applied in reference 19 to demonstrate that appropriately curved plan boundaries may lead to wings of higher lift-drag ratio than do straight-line plan boundaries.

Velocity potentials associated with discontinuous sidewash.—If the upwash field lies in the wake of the wing (fig. 5 (a)), the integration function $H(y)$ of equations (20a), (21a), and (22a) will not generally be zero (reference 15). A discontinuity in sidewash will then persist across the $z=0$ plane corresponding to the strength of the vortex sheet trailing behind the wing. The function H may be adjusted, if desired, to obtain solutions for the velocity potential that will satisfy the Kutta-Joukowski condition along subsonic trailing edges. This condition requires that for flat-plate wings the perturbation-velocity components are continuous across the trailing-edge boundary. For finite-thickness wings the velocity components must be finite at the subsonic trailing edge. The immediate problem is to establish the part of the velocity potential on the surface of the wing that is associated with the function $H(y)$.

The region $S_{D,1}$ of figure 5 that contains the vortex sheet may be temporarily considered as a portion of the wing. The virtual wing tip is then the $y=$constant line denoting the junction between the leading and trailing edges. If equation (29) is applied to the virtual wing-tip region $S_{D,1}$ of figure 5 (a), there results (in the notation of fig. 5 (b))

$$\varphi_T = -\frac{U}{M\pi} \iint_{S_{w,1}} \frac{\sigma_T \, dr \, ds}{\sqrt{(r_D - r)(s_D - s)}} - \frac{U}{M\pi} \iint_{S_{w,2}} \frac{(\sigma_B + \sigma_T) dr \, ds}{2\sqrt{(r_D - r)(s_D - s)}} - \frac{U}{M\pi} \iint_{S_{D,1}} \frac{(\lambda_0 + \lambda_H) dr \, ds}{\sqrt{(r_D - r)(s_D - s)}} \tag{54}$$

If this expression is compared with equation (20a), the result is

$$H = -\frac{U}{M\pi} \left[\iint_{S_{D,1}} \frac{(\lambda_0 + \lambda_H) dr \, ds}{\sqrt{(r_D - r)(s_D - s)}} - \iint_{S_{w,1}} \frac{(\sigma_B - \sigma_T) dr \, ds}{2\sqrt{(r_D - r)(s_D - s)}} \right] \tag{55}$$

In the notation of figure 5 (b), equation (55) may be written

$$H = -\frac{U}{M\pi} \int_{s_D}^{r_D} \frac{dr}{\sqrt{(r_D - r)}} \left[\int_{s_1(r)}^{s_2(r)} \frac{(\sigma_T - \sigma_B) ds}{2\sqrt{(s_D - s)}} + \int_{s_2(r)}^{s_D} \frac{(\lambda_0 + \lambda_H) ds}{\sqrt{s_D - s}} \right] \tag{56}$$

By use of Abel's solution (references 14, 20, or 21), equation (56) may be inverted to yield

$$\left[\int_{s_1(r)}^{s_2(r)} \frac{(\sigma_T - \sigma_B) ds}{2\sqrt{s_D - s}} + \int_{s_2(r)}^{s_D} \frac{(\lambda_0 + \lambda_H) ds}{\sqrt{s_D - s}} \right] = -\frac{M}{U} \frac{\partial}{\partial r} \int_{s_D}^{r} \frac{H\left(\frac{s_D - r_D}{M}\right) dr_D}{\sqrt{r - r_D}} \tag{56a}$$

where $H(y)$ has been expressed in oblique coordinates. Equation (56a) may be integrated by parts to give an alternative form

$$\left[\int_{s_1(r)}^{s_2(r)} \frac{(\sigma_T - \sigma_B) ds}{2\sqrt{s_D - s}} + \int_{s_2(r)}^{s_D} \frac{(\lambda_0 + \lambda_H) ds}{\sqrt{s_D - s}} \right] = -\frac{MH(0)}{U\sqrt{r - s_D}} - \frac{M}{U} \int_{s_D}^{r} \frac{\frac{\partial H}{\partial r_D} dr_D}{\sqrt{r - r_D}} \tag{56b}$$

The velocity potential at points on the wing influenced by the subsonic trailing edge (fig. 5(c)) is

$$\varphi = -\frac{U}{M\pi} \int_{s_w}^{r_2(s_w)} \frac{dr}{\sqrt{(r_w - r)}} \left[\int_{s_1(r)}^{s_2(r)} \frac{(\sigma_T - \sigma_B) ds}{2\sqrt{s_w - s}} + \int_{s_2(r)}^{s_w} \frac{(\lambda_0 + \lambda_H) ds}{\sqrt{s_w - s}} \right] - \frac{U}{M\pi} \int_{\bar{r}}^{r_2(s_w)} \frac{dr}{\sqrt{r_w - r}} \int_{s_1(r)}^{s_2(r)} \frac{(\sigma_B + \sigma_T) ds}{2\sqrt{s_w - s}} - \frac{U}{M\pi} \int_{r_2(s_w)}^{r_w} \frac{dr}{\sqrt{(r_w - r)}} \int_{s_1(r)}^{s_w} \frac{\sigma_T \, ds}{\sqrt{s_w - s}} \tag{57}$$

The second member of equation (56a) or (56b) may replace the first member along lines of constant s_D (or s_w) that extend across the wing. Equation (57) then becomes

$$\varphi = \frac{1}{\pi} \int_{s_w}^{r_2(s_w)} \frac{dr}{\sqrt{r_w - r}} \left[\frac{\partial}{\partial r} \int_{s_w}^{r} \frac{H\left(\frac{s_w - r_D}{M}\right) dr_D}{\sqrt{r - r_D}} \right] - \frac{U}{M\pi} \int_{\bar{r}}^{r_2(s_w)} \frac{dr}{\sqrt{r_w - r}} \int_{s_1(r)}^{s_2(r)} \frac{(\sigma_B + \sigma_T)}{2} \frac{ds}{\sqrt{s_w - s}} - \frac{U}{M\pi} \int_{r_2(s_w)}^{r_w} \frac{dr}{\sqrt{r_w - r}} \int_{s_1(r)}^{s_w} \frac{\sigma_T \, ds}{\sqrt{s_w - s}} \tag{58}$$

This expression reduces to equation (29) if H is zero. Inasmuch as H may be arbitrarily chosen, an infinity of solutions for regions influenced by subsonic trailing edges can satisfy the boundary conditions for thin wings at supersonic speeds. On the other hand, if the Kutta-Joukowski condition is applied, only one solution remains—the velocity potential that allows the flow to leave the subsonic trailing edge smoothly.

Once the function H is chosen, equation (56a) may be applied to evaluate the upwash (or λ) over the wing edge. The slope λ has been considered as the sum of two sets of slopes, one independent and one associated with H.

$$\lambda=\lambda_0+\lambda_H \tag{25}$$

Equation (56b) may then be written as separate equations for λ_0 and λ_H as

$$\int_{s_1(r)}^{s_2(r)}\frac{(\sigma_T-\sigma_B)ds}{2\sqrt{s_D-s}}+\int_{s_2(r)}^{s_D}\frac{\lambda_0\,ds}{\sqrt{s_D-s}}=0 \tag{27a}$$

and

$$\int_{s_2(r)}^{s_D}\frac{\lambda_H\,ds}{\sqrt{s_D-s}}=-\frac{M}{U}\frac{\partial}{\partial r}\int_{s_D}^{r}\frac{H\left(\frac{s_D-r_D}{M}\right)dr_D}{\sqrt{r-r_D}}$$

$$=-\frac{M}{U}\int_{s_D}^{r}\frac{\frac{\partial H}{\partial r_D}dr_D}{\sqrt{r-r_D}}-\frac{MH(0)}{U\sqrt{r-s_D}} \tag{59}$$

The bracket of equation (57) could thus be replaced by the first member of equation (59) if desired.

The solution of equation (27a) is obtained from equation (27d). The solution of equation (59) follows from Abel's relation and may be written in the form

$$\lambda_H=-\frac{M}{U\pi}\frac{\partial}{\partial s}\int_{s_2(r)}^{s}\frac{\left[\frac{\partial}{\partial r}\int_{s_D}^{r}\frac{H\left(\frac{s_D-r_D}{M}\right)dr_D}{\sqrt{r-r_D}}\right]ds_D}{\sqrt{s-s_D}} \tag{60}$$

This is the steady-state solution of equation (24), which could have been obtained directly. If $H(0)=0$, equation (60) may also be written as

$$\lambda_H=-\frac{M}{U\pi}\frac{\partial}{\partial s}\int_{s_2(r)}^{s}\frac{ds_D}{\sqrt{s-s_D}}\int_{s_D}^{r}\frac{\frac{\partial H}{\partial r_D}dr_D}{\sqrt{r-r_D}} \tag{60a}$$

Substitution of λ_0 from equation (27d) and λ_H from equation (60) into equation (25) yields the slopes of the upwash streamlines in the wake of the wing (region $S_{D,1}$ of fig. 5 (a)). If the region $S_{D,1}$ is treated as part of the wing, the slopes of the streamlines in the region $S_{D,2}$ may be evaluated from equation (27d). As in the derivation of equations (36a) and (37), the influence of interacting upwash fields may then be determined.

The velocity potential associated with H in equation (58) may be written in either of the alternative forms

$$\varphi_H=\frac{1}{\pi}\int_{s_w}^{r_2(s_w)}\frac{dr}{\sqrt{r_w-r}}\frac{\partial}{\partial r}\int_{s_w}^{r}\frac{H\,dr_D}{\sqrt{r-r_D}} \tag{61}$$

or

$$=\frac{2H(0)}{\pi}\tan^{-1}\sqrt{\frac{r_2-s_w}{r_w-r_2}}+\frac{1}{\pi}\int_{s_w}^{r_2(s_w)}\frac{dr}{\sqrt{r_w-r}}\int_{s_w}^{r}\frac{\frac{\partial H}{\partial r_D}dr_D}{\sqrt{r-r_D}} \tag{61a}$$

where s_w has replaced s_D as in equation (58). The question arises as to the nature of the velocity potential and the perturbation-velocity components that result from the function H, which depends only on the coordinate y. Two approaches are followed to answer this question. The first approach is to evaluate φ_H when H assumes the form of a power series. (This approach is useful for explicit evaluation of φ for wings with polynomial plan-boundary equations.) The second approach is accomplished by direct integration and differentiation without further assumptions on the form of H.

The function $H(y)=H\left(\frac{s_w-r_D}{M}\right)$ is assumed expansible in a Taylor's series of the form

$$H\left(\frac{s_w-r_D}{M}\right)=a_0+\frac{a_1(s_w-r_D)}{M}+\frac{a_2(s_w-r_D)^2}{M^2}+\cdots \tag{62}$$

(Because $H(0)$ is zero, a_0 will be zero for isolated wings.) Substitution of H from equation (62) into equation (61) yields for the velocity potential (see reference 15 for details)

$$\pi\varphi_H=2\sum_{n=0}^{\infty}\frac{\Gamma(n+1)\Gamma\left(\frac{1}{2}\right)a_n(s_w-r_w)^n}{\Gamma\left(n+\frac{1}{2}\right)M^n}\int_0^{\left(\frac{r_2-s_w}{r_w-s_w}\right)^{\frac{1}{2}}}\frac{v^{2n}dv}{\sqrt{1-v^2}} \tag{63}$$

where Γ represents the gamma function, v is an integration variable, and r_2 is a function of s_w. The integrations of equation (62) may be expressed as incomplete beta functions if desired.

The x component of the perturbation velocity that is associated with H may be obtained by differentiation of equation (63) as follows:

$$\frac{\partial\varphi_H}{\partial x}=\frac{M}{2\beta\pi}\frac{\left(\frac{dr_2}{ds_w}-1\right)}{\sqrt{r_w-r_2}}\sum_{n=0}^{\infty}\frac{(-1)^n\Gamma(n+1)\Gamma\left(\frac{1}{2}\right)a_n}{\Gamma\left(n+\frac{1}{2}\right)M^n}(r_2-s_w)^{n-\frac{1}{2}} \tag{64}$$

The infinite series is a function only of s_w for a given plan boundary and Mach number. The coefficients a_n control the strength of the vorticity in the wake of the subsonic trailing edge. The factor $\frac{\left(\frac{dr_2}{ds_w}-1\right)}{\sqrt{r_w-r_2}}$ represents an inverse square-root singularity along the wing-plan boundary that leads to an infinite pressure coefficient in the linearized theory.

The x component of the perturbation velocity in regions influenced by a subsonic trailing edge (fig. 5 (c)) is obtained as the sum of equations (64) and (44) (with a_0 set equal to zero)

$$\frac{\partial\varphi}{\partial x}=-\frac{U}{2\beta\pi}\int\int_{s_{w,1}}\frac{\left(\frac{\partial\sigma_T}{\partial r}+\frac{\partial\sigma_T}{\partial s}\right)dr\,ds}{\sqrt{(r_w-r)(s_w-s)}}-\frac{U}{4\beta\pi}\int\int_{s_{w,2}}\frac{\left[\frac{\partial(\sigma_B+\sigma_T)}{\partial r}+\frac{\partial(\sigma_B+\sigma_T)}{\partial s}\right]dr\,ds}{\sqrt{(r_w-r)(s_w-s)}}-\frac{U}{2\beta\pi}\int_{ab}\frac{\sigma_T(ds-dr)}{\sqrt{(r_w-r)(s_w-s)}}-\frac{U}{2\beta\pi}\int_{bod}\frac{(\sigma_B+\sigma_T)(ds-dr)}{2\sqrt{(r_w-r)(s_w-s)}}$$
$$\frac{U}{4\beta\pi}\frac{\left(1-\frac{dr_2}{ds_w}\right)}{\sqrt{r_w-r_2}}\left[\int_{bd}\frac{(\sigma_T-\sigma_B)ds}{\sqrt{s_w-s}}+\frac{2M}{U}\sum_{n=1}^{\infty}\frac{(-1)^n\Gamma(n+1)\Gamma\left(\frac{1}{2}\right)a_n(r_2-s_w)^{n-\frac{1}{2}}}{\Gamma\left(n+\frac{1}{2}\right)M^n}\right] \tag{65}$$

For flat-plate wings, $\sigma_B=-\sigma_T=\alpha$ and equation (65) becomes

$$\frac{\partial\varphi}{\partial x}=\frac{U\alpha}{2\beta\pi}\int_{ab}\frac{(ds-dr)}{\sqrt{(r_w-r)(s_w-s)}}+\frac{U\alpha}{\beta\pi}\frac{\left(1-\frac{dr_2}{ds_w}\right)}{\sqrt{r_w-r_2}}\left[\sqrt{s_w-s_1(r_2)}-\frac{M}{2U\alpha}\sum_{n=1}^{\infty}\frac{(-1)^n\Gamma(n+1)\Gamma\left(\frac{1}{2}\right)a_n(r_2-s_w)^{n-\frac{1}{2}}}{\Gamma\left(n+\frac{1}{2}\right)M^n}\right] \tag{66}$$

or

$$\frac{\partial\varphi}{\partial x}=\frac{U\alpha}{2\beta\pi}\int_{ab}\frac{ds-dr}{\sqrt{(r_w-r)(s_w-s)}}+\frac{\left(1-\frac{dr_2}{ds_w}\right)g(s_w)}{\sqrt{r_w-r_2}} \tag{66a}$$

where $g(s_w)$ represents $\frac{U\alpha}{\beta\pi}$ times the bracketed part of equation (66). The quantity $\left(1-\frac{dr_2}{ds_w}\right)g(s_w)$ is constant along lines of constant s_w, so that the strength of the shed vorticity could feasibly be experimentally determined by a single pressure measurement on the wing surface for each value of s_w.

If the Kutta-Joukowski condition is to be satisfied for antisymmetric wings, all three of the perturbation-velocity components must be continuous across the subsonic trailing edge. Continuity in any one of the three components will evaluate the coefficients a_n and assure the continuity of the other two. Continuity of $\frac{\partial\varphi}{\partial x}$ across the subsonic trailing edge for flat-plate wings, covered by equation (66a) for example, requires that $g(s_w)=0$. The solution that satisfies the Kutta-Joukowski condition is thus

$$\frac{\partial\varphi}{\partial x}=\frac{U\alpha}{2\beta\pi}\int_{ab}\frac{ds-dr}{\sqrt{(r_w-r)(s_w-s)}} \tag{67}$$

The coefficients $a_1, a_2, \ldots a_n$ may be evaluated by the relation $g(s_w)=0$, or for flat-plate wings,

$$\sqrt{s_w-s_1(r_2)}=\frac{M}{2U\alpha}\sum_{n=1}^{\infty}\frac{(-1)^n\Gamma(n+1)\Gamma\left(\frac{1}{2}\right)a_n}{\Gamma\left(n+\frac{1}{2}\right)M^n}p^{2n-1} \tag{68}$$

where $p=\sqrt{r_2-s_w}$. Equation (68) is a power series in p whose nth coefficient a_n may be evaluated in terms of the $(2n-1)$th derivative about $p=0$. Because the first member of equation (68) is finite when $p=0$, $a_0=0$ as previously stated. Differentiation of the first member of equation (68) can be accomplished by successive applications of the relation

$$\frac{d}{dp}=\frac{2\sqrt{r_2-s_w}}{\left(\frac{dr_2}{ds_w}-1\right)}\frac{d}{ds_w} \tag{69}$$

By application of equation (69) and L'Hospital's rule to equation (68), the coefficients a_1 and a_2, for example, are given as

$$a_1=-U\alpha\sqrt{\frac{1-\frac{ds_1}{dr_2}\frac{dr_2}{ds_w}}{\frac{dr_2}{ds_w}-1}} \tag{70}$$

evaluated at $r_2=s_w=0$.

$$a_2=\frac{MU\alpha}{2}\left(1-\frac{ds_1}{dr_2}\frac{dr_2}{ds_w}\right)^{\frac{1}{2}}\frac{d^2r_2}{ds_w^2}\left[\left(\frac{dr_2}{ds_w}-1\right)^{-\frac{5}{2}}-\left(\frac{dr_2}{ds_w}-1\right)^{-\frac{3}{2}}-\frac{3}{8}\left(\frac{dr_2}{ds_w}-1\right)\right]-$$
$$\frac{MU\alpha}{2}\left(1-\frac{ds_1}{dr_2}\frac{dr_2}{ds_w}\right)^{-\frac{1}{2}}\left[\frac{d^2s_1}{dr_2^2}\left(\frac{dr_2}{ds_w}\right)^2+\frac{ds_1}{dr_2}\frac{d^2r_2}{ds_w^2}\right]\left[\left(\frac{dr_2}{ds_w}-1\right)^{\frac{1}{2}}-\left(\frac{dr_2}{ds_w}-1\right)^{-\frac{1}{2}}-\frac{3}{8}\left(1-\frac{ds_1}{dr_2}\frac{dr_2}{ds_w}\right)\right] \tag{71}$$

evaluated at $r_2=s_w=0$. The other coefficients may be similarly evaluated. If wings with straight-line plan boundaries are considered (as for conical flow wings), all the coefficients $a_1, a_2, a_3, \ldots a_n$ except the first are zero. For curved plan boundaries, higher-order terms in the series expansion for H are generally required to satisfy the Kutta-Joukowski condition. The expressions (70) and (71), which determine the first two coefficients in the series expansion (equation (62)), are unbounded if $\frac{dr_2}{ds_w}$ approaches unity at the origin.

Once the coefficients $a_1, a_2, a_3, \ldots a_n$ have been determined, the velocity potential and its partial derivative with respect to x are given by equations (63) and (64), respectively. The y component of the perturbation velocity is obtained by partial differentiation of equation (63).

The z component of the perturbation velocity associated with the function H may be obtained by substituting equation (62) in equation (60) ($a_0=0$):

$$\frac{1}{U}\left(\frac{\partial\varphi}{\partial z}\right)_H=\lambda_H=\frac{M}{U\pi(s-s_2)^{\frac{1}{2}}}\left[\frac{a_1(r-s_2)^{\frac{1}{2}}}{M\times\frac{1}{2}}-\frac{a_2 2\times1(r-s_2)^{\frac{3}{2}}}{M^2\times\frac{3}{2}\times\frac{1}{2}}+\frac{a_3 3\times2\times1(r-s_2)^{\frac{5}{2}}}{M^3\times\frac{5}{2}\times\frac{3}{2}\times\frac{1}{2}}-\cdots\right]-$$

$$\frac{2M}{U\pi}\log_e\frac{\sqrt{r-s_2}+\sqrt{s-s_2}}{\sqrt{r-s}}\left[\frac{a_1}{M}-\frac{2a_2(r-s)}{M^2}+\frac{3a_3}{M^3}(r-s)^2-\frac{4a_4}{M^4}(r-s)^3\cdots\right]+$$

$$\frac{M}{U\pi}(s-s_2)^{\frac{1}{2}}(r-s_2)^{\frac{1}{2}}\left\{\frac{a_2}{M^2}\frac{2\times1}{\frac{1}{2}}-\frac{a_3}{M^3}\frac{3\times2\times1}{\frac{3}{2}\times\frac{1}{2}}\left[(r-s_2)\frac{1}{2}+\frac{3}{2}\times\frac{1}{2}(r-s)\right]+\right.$$

$$\frac{a_4}{M^4}\frac{4\times3\times2\times1}{\frac{5}{2}\times\frac{3}{2}\times\frac{1}{2}}\left[\frac{(r-s_2)^2}{3}+\frac{\frac{5}{2}(r-s_2)(r-s)}{3\times2}+\frac{\frac{5}{2}\times\frac{3}{2}(r-s)^2}{3\times2\times1}\right]-$$

$$\left.\frac{a_5}{M^5}\frac{5\times4\times3\times2\times1}{\frac{7}{2}\times\frac{5}{2}\times\frac{3}{2}\times\frac{1}{2}}\left[\frac{(r-s_2)^3}{4}+\frac{\frac{7}{2}(r-s_2)^2(r-s)}{4\times3}+\frac{\frac{7}{2}\times\frac{5}{2}(r-s_2)(r-s)^2}{4\times3\times2}+\frac{\frac{7}{2}\times\frac{5}{2}\times\frac{3}{2}(r-s)^3}{4\times3\times2\times1}\right]+\cdots\right\}+\cdots \quad (72)$$

The terms factored by $a_2, a_3, a_4, \ldots a_n$ do not appear for wings with straight-line plan boundaries.

An alternative approach to the determination of the form for the perturbation-velocity components associated with the function H may be obtained by integration and differentiation of equation (61a). This manipulation is accomplished by interchanging the order of integration with respect to r and r_D, which of course alters the limits of integration, giving

$$\varphi_H=\frac{2H(0)}{\pi}\tan^{-1}\sqrt{\frac{r_2-s_w}{r_w-r_2}}+$$

$$\frac{1}{\pi}\int_{s_w}^{r_2(s_w)}\frac{\partial H}{\partial r_D}dr_D\int_{r_D}^{r_2(s_w)}\frac{dr}{\sqrt{(r_w-r)(r-r_D)}} \quad (61b)$$

or

$$\varphi_H=\frac{2H(0)}{\pi}\tan^{-1}\sqrt{\frac{r_2-s_w}{r_w-r_2}}+\frac{2}{\pi}\int_{s_w}^{r_2(s_w)}\frac{\partial H}{\partial r_D}\tan^{-1}\sqrt{\frac{r_2-r_D}{r_w-r_2}}dr_D \quad (61c)$$

Equation (61c) may be integrated by parts to give the alternative form

$$\varphi_H=\frac{\sqrt{r_w-r_2}}{\pi}\int_{s_w}^{r_2(s_w)}\frac{H\,dr_D}{(r_w-r_D)\sqrt{r_2-r_D}} \quad (61d)$$

Thus, either by equation (61c) or equation (61d), φ_H is evaluated by a line integral across the vortex field along the constant s_w Mach line.

The x and y components of the perturbation velocity may be obtained by differentiation of equation (61c).

$$\frac{2\beta}{M}\frac{\partial\varphi_H}{\partial x}=\frac{H(0)\left(\frac{dr_2}{ds_w}-1\right)}{\pi\sqrt{(r_w-r_2)(r_2-s_w)}}-\frac{2}{\pi}\tan^{-1}\sqrt{\frac{r_2-s_w}{r_w-r_2}}\left(\frac{\partial H}{\partial r_D}\right)_{r_D=s_w}+$$

$$\frac{2}{\pi}\int_{s_w}^{r_2(s_w)}\left(\frac{\partial}{\partial r_w}+\frac{\partial}{\partial s_w}\right)\left(\frac{\partial H}{\partial r_D}\tan^{-1}\sqrt{\frac{r_2-r_D}{r_w-r_2}}\right)dr_D \quad (73)$$

If equation (73) is rewritten, with the use of the identity

$$\left(\frac{\partial}{\partial r_w}+\frac{\partial}{\partial s_w}\right)\frac{\partial H}{\partial r_D}=-\frac{\partial^2 H}{\partial r_D^2}$$

there results

$$\frac{2\beta}{M}\frac{\partial\varphi_H}{\partial x}=\frac{H(0)\left(\frac{dr_2}{ds_w}-1\right)}{\pi\sqrt{(r_w-r_2)(r_2-s_w)}}-\frac{2}{\pi}\tan^{-1}\sqrt{\frac{r_2-s_w}{r_w-r_2}}\left(\frac{\partial H}{\partial r_D}\right)_{r_D=s_w}+$$

$$\frac{2}{\pi}\int_{s_w}^{r_2(s_w)}\frac{\partial H}{\partial r_D}\left(\frac{\partial}{\partial r_w}+\frac{\partial}{\partial s_w}\right)\tan^{-1}\sqrt{\frac{r_2-r_D}{r_w-r_2}}dr_D-$$

$$\frac{2}{\pi}\int_{s_w}^{r_2(s_w)}\frac{\partial^2 H}{\partial r_D^2}\tan^{-1}\sqrt{\frac{r_2-r_D}{r_w-r_2}}dr_D \quad (73a)$$

Integration by parts of the fourth term in the second member of equation (73a) leaves

$$\frac{2\beta}{M}\frac{\partial\varphi_H}{\partial x}=\frac{H(0)\left(\frac{dr_2}{ds_w}-1\right)}{\pi\sqrt{(r_w-r_2)(r_2-s_w)}}+$$

$$\frac{2}{\pi}\int_{s_w}^{r_2(s_w)}\frac{\partial H}{\partial r_D}\left[\left(\frac{\partial}{\partial r_w}+\frac{\partial}{\partial s_w}+\frac{\partial}{\partial r_D}\right)\tan^{-1}\sqrt{\frac{r_2-r_D}{r_w-r_2}}\right]dr_D$$

or

$$\frac{\partial\varphi_H}{\partial x}=\frac{M\left(\frac{dr_2}{ds_w}-1\right)}{2\beta\pi\sqrt{r_w-r_2}}\left[\frac{H(0)}{\sqrt{r_2-s_w}}+\int_{s_w}^{r_2(s_w)}\frac{\frac{\partial H}{\partial r_D}dr_D}{\sqrt{r_2-r_D}}\right] \quad (73b)$$

(The series of equation (64) may be obtained from equations (73b) and (62) by successive integration of equation (73b) by parts.) In a similar manner,

$$\frac{2}{M}\frac{\partial\varphi_H}{\partial y}=\frac{H(0)\left(\frac{dr_2}{ds_w}+1\right)}{\pi\sqrt{(r_w-r_2)(r_2-s_w)}}-\frac{2H(0)\sqrt{r_w-r_2}}{\pi(r_w-s_w)\sqrt{r_2-s_w}}+$$

$$\frac{2}{\pi}\int_{s_w}^{r_2(s_w)}\frac{\partial H}{\partial r_D}\left[\left(\frac{\partial}{\partial s_w}-\frac{\partial}{\partial r_w}+\frac{\partial}{\partial r_D}\right)\tan^{-1}\sqrt{\frac{r_2-r_D}{r_w-r_2}}\right]dr_D \quad (74)$$

or

$$\frac{\partial \varphi_H}{\partial y}=\frac{M\left(1+\frac{dr_2}{ds_w}\right)}{2\pi\sqrt{r_w-r_2}}\left[\frac{H(0)}{\sqrt{r_2-s_w}}+\int_{s_w}^{r_2(s_w)}\frac{\frac{\partial H}{\partial r_D}dr_D}{\sqrt{r_2-r_D}}\right]-\frac{M\sqrt{r_w-r_2}}{\pi}\left[\frac{H(0)}{(r_w-s_w)\sqrt{r_2-s_w}}+\int_{s_w}^{r_2(s_w)}\frac{\frac{\partial H}{\partial r_D}dr_D}{(r_w-r_D)\sqrt{r_2-r_D}}\right] \tag{74a}$$

Thus the perturbation-velocity components (associated with H) on the surface of the wing are given by simple line integrals across the vortex field along the constant s_w Mach line. For a given wing plan, the line integral of equation (73b) (and the first line integral of equation (74a)) is a function only of the shed vorticity and of the coordinate s_w (as was similarly noted for equation (64)). The form of equation (73b) suggests that the equation might be more general than the example for which it was derived.

If the Kutta-Joukowski condition is to be satisfied along the subsonic trailing edge, the value of $\frac{\partial H}{\partial r_D}$ that appears in equations (60a), (61a), (73), and (74) must satisfy the integral equation

$$\frac{H(0)}{\sqrt{r_2-s_w}}+\int_{s_w}^{r_2(s_w)}\frac{\frac{\partial H}{\partial r_D}dr_D}{\sqrt{r_2-r_D}}=\frac{U}{M}\int_{\text{bd}}\frac{(\sigma_B-\sigma_T)ds}{2\sqrt{s_w-s}} \tag{75}$$

where σ depends on $r_2(s_w)$ and s. This expression results from adding the terms of equations (44) and (73b) that give infinite values of $\frac{\partial \varphi}{\partial x}$ along the subsonic trailing edge (that is, those terms that contain the factor $\left(\frac{dr_2}{ds_w}-1\right)\Big/\sqrt{r_w-r_2}$) and equating these terms to zero. An alternative evaluation of H may be obtained from equation (22a) and the known values of φ or $\frac{\partial \varphi}{\partial x}$ for solutions satisfying the Kutta-Joukowski condition

$$2H=\varphi_T-\varphi_B=\int_{-\infty}^{x_2(y)}\left(\frac{\partial \varphi_T}{\partial x}-\frac{\partial \varphi_B}{\partial x}\right)dx \tag{76}$$

If in equation (76), φ_T and φ_B are divided into those components associated with and independent of H (as in equation (58)), only the part associated with H remains after the subtraction. The part associated with H is zero from $-\infty$ up to the $s_w=0$ Mach line and has the value (from equations (73b) and (75))

$$\frac{\partial \varphi_H}{\partial x}=\pm\frac{U\left(\frac{dr_2}{ds_w}-1\right)}{2\beta\pi\sqrt{r_w-r_2}}\int_{\text{bd}}\frac{(\sigma_B-\sigma_T)ds}{2\sqrt{s_w-s}} \tag{77}$$

from the $s_w=0$ Mach line to the subsonic trailing edge. (The + or the − sign is used for the top or bottom wing surface, respectively.) Application of the transformation equations (16) for constant values of y (which infers that $dr_w=ds_w$) to equations (76) and (77) then gives

$$H=\frac{U}{M\pi}\int_0^{\frac{M}{2\beta}(x_2+\beta y)}\frac{\left(\frac{dr_2}{ds_w}-1\right)ds_w}{\sqrt{s_w-My-r_2}}\int_{s_1(r_2)}^{s_w}\frac{(\sigma_B-\sigma_T)ds}{2\sqrt{s_w-s}} \tag{78}$$

where x_2 represents the plan-boundary equation $x=x_2(y)$. This value of H may then be inserted in equations (60) and (74) to complete the evaluation of perturbation-velocity components associated with the discontinuity of sidewash behind subsonic (or supersonic) trailing edges.

Acceleration-potential derivation of solutions satisfying Kutta-Joukowski condition.—Additional insight into the origin of pressure forces may be gained by deriving the expressions for the influence of the upwash field in terms of the acceleration potential $\frac{\partial \varphi}{\partial x}$ rather than φ. This derivation may proceed either from equation (42a) and figure 4 (a) or from equation (44) and figure 5 (b) under the assumption that λ is finite along the wing boundary in conformance with the Kutta-Joukowski condition. Both derivations yield the same result, but the second approach is simpler to justify. If equation (44) is applied to the virtual wing region $S_{D,1}$ of figure 5 (b) for both top and bottom surfaces, there results

$$\frac{\partial(\varphi_T-\varphi_B)}{\partial x}=-\frac{U}{2\beta\pi}\int_{s_2}^{r_w}\frac{dr}{\sqrt{r_w-r}}\left\{\int_{s_1(r)}^{s_2(r)}\frac{\left[\frac{\partial(\sigma_T-\sigma_B)}{\partial r}+\frac{\partial(\sigma_T-\sigma_B)}{\partial s}\right]ds}{\sqrt{s_w-s}}+\int_{s_2(r)}^{s_w}\frac{2\left(\frac{\partial\lambda}{\partial r}+\frac{\partial\lambda}{\partial s}\right)ds}{\sqrt{s_w-s}}+\frac{(\sigma_B-\sigma_T)_1\left(\frac{ds_1}{dr}-1\right)}{\sqrt{s_w-s_1(r)}}+\frac{(\sigma_T-\sigma_B)_2\left(\frac{ds_2}{dr}-1\right)}{\sqrt{s_w-s_2(r)}}-\frac{2\lambda_2\left(\frac{ds_2}{dr}-1\right)}{\sqrt{s_w-s_2(r)}}\right\}=0 \tag{79}$$

The last two terms arise in the evaluation of the surface integral from the discontinuity of streamline slopes along the trailing edge. Inasmuch as equation (79) holds for all values of r_w, there results

$$\int_{s_1(r)}^{s_w}\frac{\left(\frac{\partial\lambda}{\partial r}+\frac{\partial\lambda}{\partial s}\right)ds}{\sqrt{s_w-s}}-\frac{\lambda\left(\frac{ds_2}{dr}-1\right)}{\sqrt{s_w-s_2(r)}}=\int_{s_1(r)}^{s_2(r)}\frac{\frac{1}{2}\left[\frac{\partial(\sigma_B-\sigma_T)}{\partial r}+\frac{\partial(\sigma_B-\sigma_T)}{\partial s}\right]ds}{\sqrt{s_w-s}}+\frac{(\sigma_T-\sigma_B)_1}{2}\frac{\left(\frac{ds_1}{dr}-1\right)}{\sqrt{s_w-s_1(r)}}+\frac{(\sigma_B-\sigma_T)_2\left(\frac{ds_2}{dr}-1\right)}{2\sqrt{s_w-s_2(r)}} \tag{79a}$$

(If equation (27a) is differentiated partially with respect to r and s_D, addition of the two resulting equations gives equation (79a). Inasmuch as equation (27a) excludes the effects of shed vorticity whereas equation (79a) does not,

the inference may be drawn that equation (27a) could include the effects of shed vorticity for time-independent cases by the addition of a function of $r-s_D$. This fact was shown in another manner in reference 15.) With reference to figure 5 (c), $\frac{\partial\varphi}{\partial x}$ on the surface of the wing is

$$\frac{\partial\varphi}{\partial x}=-\frac{U}{2\beta\pi}\int\int_{S_{w,1}}\frac{\left(\frac{\partial\sigma_T}{\partial r}+\frac{\partial\sigma_T}{\partial s}\right)dr\,ds}{\sqrt{(r_w-r)(s_w-s)}}-\frac{U}{2\beta\pi}\int_{ab}\frac{\sigma_T(ds-dr)}{\sqrt{(r_w-r)(s_w-s)}}-\frac{U}{2\beta\pi}\int_{b'0d'}\frac{(\sigma_B+\sigma_T)(ds-dr)}{2\sqrt{(r_w-r)(s_w-s)}}-$$

$$\frac{U}{2\beta\pi}\int\int_{S_{w,2'}}\frac{\frac{1}{2}\left[\frac{\partial(\sigma_B+\sigma_T)}{\partial r}+\frac{\partial(\sigma_B+\sigma_T)}{\partial s}\right]dr\,ds}{\sqrt{(r_w-r)(s_w-s)}}-$$

$$\frac{U}{2\beta\pi}\int_{s_w}^{r_2(s_w)}\frac{dr}{\sqrt{r_w-r}}\left[\int_{s_1(r)}^{s_2(r)}\frac{\left(\frac{\partial\sigma_T}{\partial r}+\frac{\partial\sigma_T}{\partial s}\right)ds}{\sqrt{s_w-s}}-\frac{\sigma_T\left(\frac{ds_1}{dr}-1\right)}{\sqrt{s_w-s_1(r)}}+\frac{\sigma_T\left(\frac{ds_2}{dr}-1\right)}{\sqrt{s_w-s_2(r)}}+\int_{s_2(r)}^{s_w}\frac{\left(\frac{\partial\lambda}{\partial r}+\frac{\partial\lambda}{\partial s}\right)ds}{\sqrt{s_w-s}}-\frac{\lambda_2\left(\frac{ds_2(r)}{dr}-1\right)}{\sqrt{s_w-s_2(r)}}\right] \tag{80}$$

Elimination of λ from equations (79a) and (80) gives

$$\frac{\partial\varphi}{\partial x}=-\frac{U}{2\beta\pi}\int\int_{S_{w,1}}\frac{\left(\frac{\partial\sigma_T}{\partial r}+\frac{\partial\sigma_T}{\partial s}\right)dr\,ds}{\sqrt{(r_w-r)(s_w-s)}}-$$

$$\frac{U}{2\beta\pi}\int\int_{S_{w,2}}\frac{\frac{1}{2}\left[\frac{\partial(\sigma_B+\sigma_T)}{\partial r}+\frac{\partial(\sigma_B+\sigma_T)}{\partial s}\right]dr\,ds}{\sqrt{(r_w-r)(s_w-s)}}-$$

$$\frac{U}{2\beta\pi}\int_{ab}\frac{\sigma_T(ds-dr)}{\sqrt{(r_w-r)(s_w-s)}}-$$

$$\frac{U}{2\beta\pi}\int_{bcd}\frac{(\sigma_B+\sigma_T)(ds-dr)}{2\sqrt{(r_w-r)(s_w-s)}} \tag{80a}$$

Equation (80a) is the same as equation (65) except that the term generating infinite loads along the wing-plan boundary is missing. Thus, when the brace of equation (65) is zero, the Kutta-Joukowski condition applies and equation (80a) results. The vorticity in the wake of the wing under such circumstances is of sufficient strength to cancel the contribution to $\frac{\partial\varphi}{\partial x}$ of the line integral along bd.

Three approaches have been presented to show that the Kutta-Joukowski condition can be formally satisfied along subsonic trailing edges of thin wings at supersonic speeds. Each of these approaches implies a discontinuity in sidewash (that is, a vortex sheet) behind the wing of sufficient strength to cancel the term in equation (44) evaluated by the line integral along bd. This term appears to depend only on those wing slopes lying on bd, which can only influence the flow field along or downstream of this Mach line. On the other hand, the contribution of the function H, which opposes this integral for Kutta condition solutions (equation (75)), is determined by the discontinuity in sidewash established upstream of this Mach line (except for the isolated point d). The implication is that the Kutta-Joukowski condition cannot be satisfied without an interchange of cause and effect. Once the flow is established, however, the boundary conditions may be satisfied by solutions fulfilling the Kutta-Joukowski condition. Application of the Kutta-Joukowski condition would seem to imply at least one of the following: (a) Downstream disturbances might be felt upstream through the wake of the wing or through the boundary layer whether initially or continuously. The apparent interchange of cause and effect in the linearized calculation would then be negated; (b) only the vortex line from the point d contributes to $\frac{\partial\varphi}{\partial x}$ along the line s_w (This argument seems to be in opposition to equation (73b).); (c) the wing slopes must change continuously in approaching the line bd (as they would if they were represented by a power series) so that the apparent independence of the line integral of forward wing slopes might not be real. The application of the Kutta-Joukowski condition at supersonic speeds is still an open question, which should be determined by experiment.

In order to illustrate the Kutta-Joukowski solutions, the perturbation-velocity components of a thin, flat, trapezoidal wing with a subsonic trailing edge on the tip may be derived. The wing equations are $s=-k_1r$ and $s=k_2r$. Either by integration of equation (67) or when the singular term of equation (48) is dropped, $\frac{\partial\varphi}{\partial x}$ may be derived as

$$\frac{\partial\varphi}{\partial x}=\frac{U\alpha}{\beta\pi}\frac{(k_1+1)}{\sqrt{k_1}}\tan^{-1}\sqrt{\frac{k_1(k_2r_w-s_w)}{(k_1+k_2)s_w}} \tag{81}$$

(Equations (78) and (73b) also lead to equation (81) for this example.) From equation (70),

$$a_1=-U\alpha\sqrt{\frac{k_1+k_2}{1-k_2}}$$

$$a_2=a_3=\ldots=a_n=0$$

This value may be inserted in equations (62) and (63). Addition of $\frac{\partial\varphi_H}{\partial y}$ calculated from equation (63) or (74a) and $\frac{\partial\varphi}{\partial y}$ from equation (49) gives

$$\frac{\partial\varphi}{\partial y}=\frac{U\alpha}{\pi}\left[\frac{(1-k_1)}{\sqrt{k_1}}\tan^{-1}\sqrt{\frac{k_1(k_2r_w-s_w)}{(k_1+k_2)s_w}}-\right.$$

$$\left.2\sqrt{\frac{k_1+k_2}{1-k_2}}\tan^{-1}\sqrt{\frac{s_w(1-k_2)}{k_2r_w-s_w}}\right] \tag{82}$$

Likewise, from equations (72) and (27e),

$$\lambda=\frac{1}{U}\frac{\partial\varphi}{\partial z}=-\frac{2\alpha}{\pi}\left[\tan^{-1}\sqrt{\frac{r(k_1+k_2)}{s-k_2r}}+\right.$$

$$\left.\sqrt{\frac{k_1+k_2}{1-k_2}}\log_e\frac{\sqrt{r-s}}{\sqrt{s-k_2r}+\sqrt{r(1-k_2)}}\right] \tag{83}$$

for

$$k_2<\frac{s}{r}\leq 1$$

The values of the perturbation velocities, equations (81) to (83), are constant along radial lines from the origin showing that the flow is conical. This fact resulted from the use of straight-line plan boundaries, but was not otherwise assumed in the derivation of the perturbation-velocity components.

Circulation and lift.—As in subsonic-wing theory, the lift per unit span is directly related to the circulation, as shown in reference 25. The lift increment per unit span $\frac{dL}{dy}$ is given as

$$\frac{dL}{dy}=\frac{1}{2}\rho U^2\int_{-\infty}^{x_t}(C_{p,B}-C_{p,T})dx$$
$$=-\rho U\int_{-\infty}^{x_t}\left(\frac{\partial\varphi_B}{\partial x}-\frac{\partial\varphi_T}{\partial x}\right)dx \qquad (84)$$

where the subscript t indicates along the trailing edge. Integration of equation (84) gives

$$\frac{dL}{dy}=-\rho U(\varphi_B-\varphi_T)_t=2\rho UH(y)=\rho U\Gamma \qquad (84a)$$

where Γ is the circulation evaluated along a wing chord. Equation (84a) is the familiar subsonic relation and may be used to evaluate experimental wing lifts from wake measurements, or to evaluate the theoretical lift of a wing as a line integral across the span. The velocity potential along the trailing edge is, of course, a function only of y, x having been eliminated by means of the trailing-edge boundary equation.

Computed examples of perturbation-velocity components.—The theoretical expressions for the velocity potential near thin wings at supersonic speeds describe the flow characteristics. The nature of these flows may be clarified by numerical examples for flat-plate wings. The perturbation-velocity components in regions influenced by the tip of a trapezoidal wing are computed to illustrate the effects of subsonic leading and trailing edges. In addition, load distributions associated with angle of attack, uniform pitch, and uniform roll are illustrated for a complete wing.

The effects of subsonic leading edges on the perturbation-velocity components may be illustrated for the trapezoidal wing of figure 13 (a). The supersonic and subsonic leading edges are defined by the equations $s_1=-\frac{r}{2}$ and $s_2=2r$. If these values are substituted into equations (48), (49), and (27e), the perturbation-velocity components in the $z=0$ plane are obtained. These components are presented in figure 14.

The two addends that give $\frac{\partial\varphi}{\partial x}$ and $\frac{\partial\varphi}{\partial y}$ are also included on figures 14 (a) and 14 (b). The arc-tangent expression controls the value of these two velocity components near the Mach line from the subsonic and supersonic leading-edge intersection, but the inverse square-root singularity becomes increasingly important near the wing tip.

The value of $\frac{\partial\varphi}{\partial x}$ rapidly changes near the innermost Mach line from the origin, reaches an extreme, and then becomes unbounded near the tip. The quantity $\frac{\partial\varphi}{\partial y}$, on the other hand, changes monotonically from a positive value on the innermost Mach line to an unbounded negative value along the tip. The value of $\frac{\partial\varphi}{\partial z}$ (fig. 14 (c)) is likewise unbounded in the upwash field in the vicinity of the wing tip, but rapidly drops as $\frac{\beta y}{x}$ increases. The upwash is zero along the outermost Mach line from the origin.

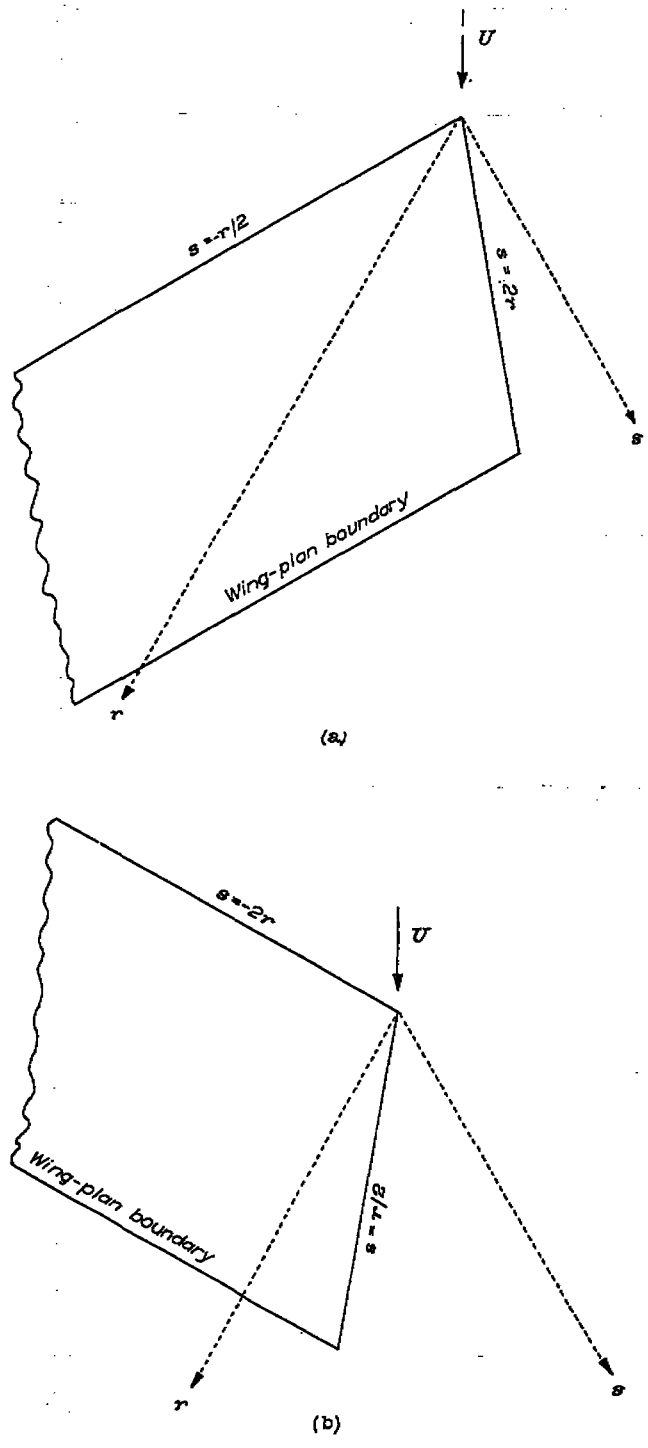

(a) Subsonic leading edge.

(b) Subsonic trailing edge.

FIGURE 13.—Trapezoidal-wing plan forms.

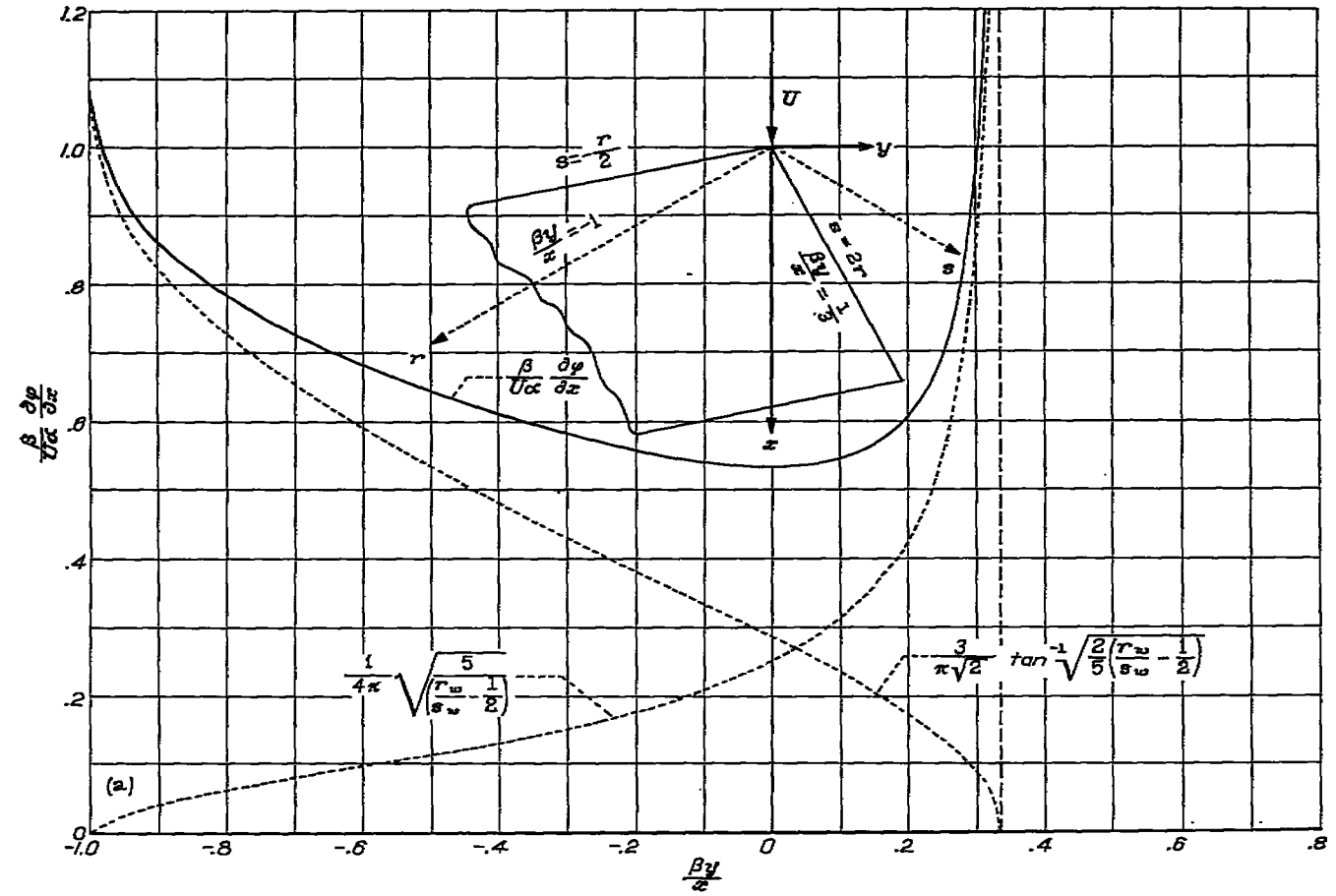

(a) x component.

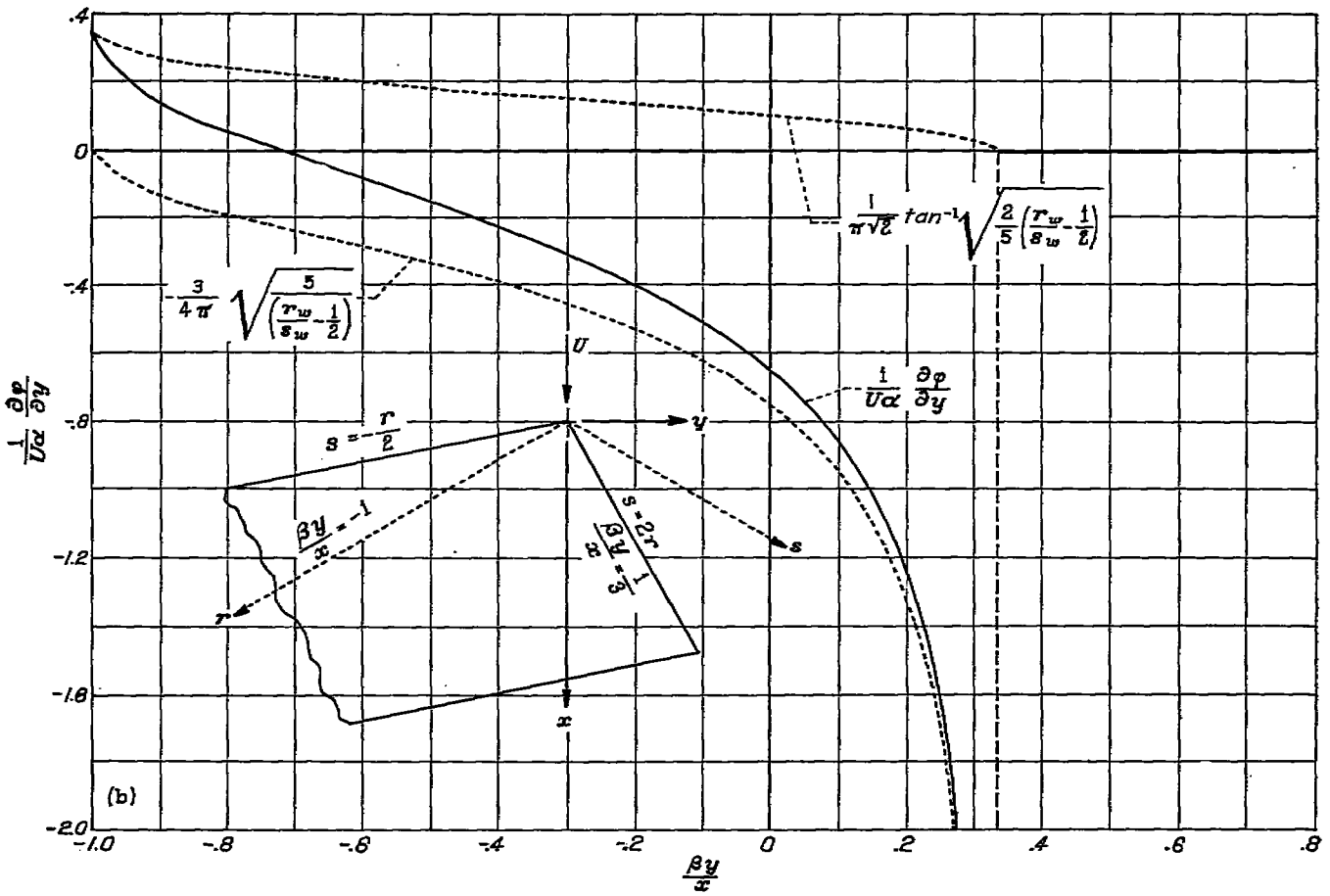

(b) y component.

FIGURE 14.—Perturbation velocities near tip of trapezoidal wing with subsonic leading edge.

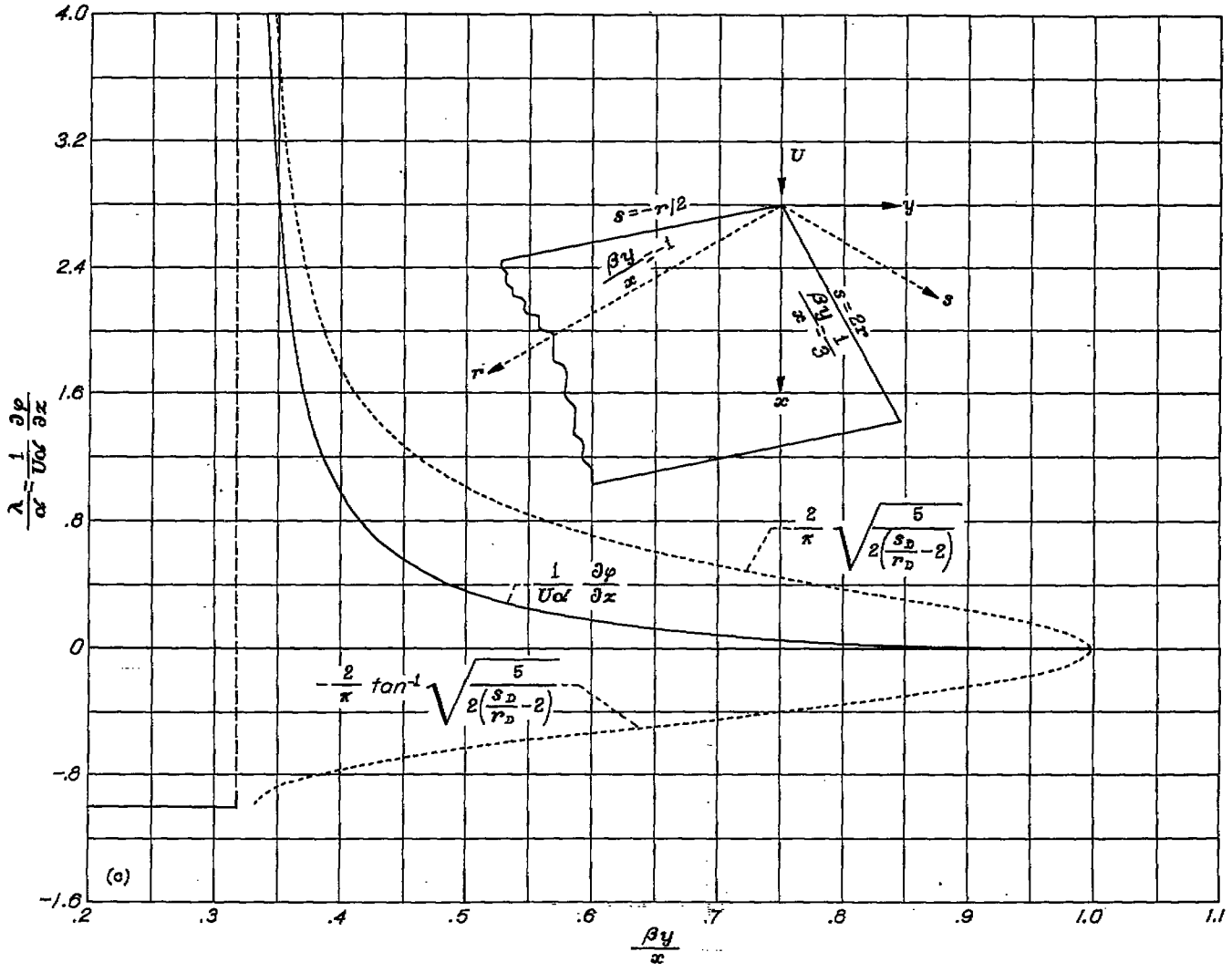

(c) z component.

FIGURE 14.—Concluded. Perturbation velocities near tip of trapezoidal wing with subsonic leading edge.

If the trapezoidal wing is flown backwards, the equations for the wing boundaries are $s_1=-2r$ and $s_2=0.5r$. In this case the wing tip is a subsonic trailing edge for which the Kutta-Joukowski condition may be (arbitrarily) imposed. The three perturbation-velocity components, which were calculated by equations (81) to (83), are presented in figure 15.

Both $\frac{\partial\varphi}{\partial x}$ and $\frac{\partial\varphi}{\partial y}$ monotonically change from the two-dimensional regions to the wing tip. In the upwash field $-\frac{1}{3}<\frac{\beta y}{x}<0$, $\frac{\partial\varphi}{\partial x}$ is zero and $\frac{\partial\varphi}{\partial y}$ is constant, corresponding to a constant strength of vorticity in the wake of the wing. The velocity component $\frac{\partial\varphi}{\partial z}$ is constant across the wing, then monotonically increases in the upwash field from the value along the wing tip to infinity along the line $\frac{\beta y}{x}=0$ (corresponding to the limiting vortex line).

Many of the equations presented heretofore are given in terms of the wing slopes σ. These slopes, however, are related to the induced z component of the perturbation velocity by equation (19). The formulations are equally valid when w is induced by either steady wing motions or by wing geometry. The effective wing slopes on a flat-plate wing associated with lift, uniform roll, and uniform pitch are, for example,

$$\left.\begin{array}{lll} \text{lift:} & & \\ & \sigma_T=-\alpha & \sigma_B=\alpha \\ \text{roll:} & & \\ & \sigma_T=-\frac{w}{U}=-\frac{m}{U}(\eta-\eta_0) & \sigma_B=\frac{m}{U}(\eta-\eta_0) \\ \text{pitch:} & & \\ & \sigma_T=-\frac{w}{U}=-\frac{n}{U}(\xi-\xi_0) & \sigma_B=\frac{n}{U}(\xi-\xi_0) \end{array}\right\} \quad (85)$$

where m and n are the rates of roll and pitch and η_0 and ξ_0 are the coordinate distances to the roll and pitch axes, respectively. If these wing slopes are substituted in equations such as equation (44), the load distributions associated with lift, steady roll, and steady pitch may be determined.

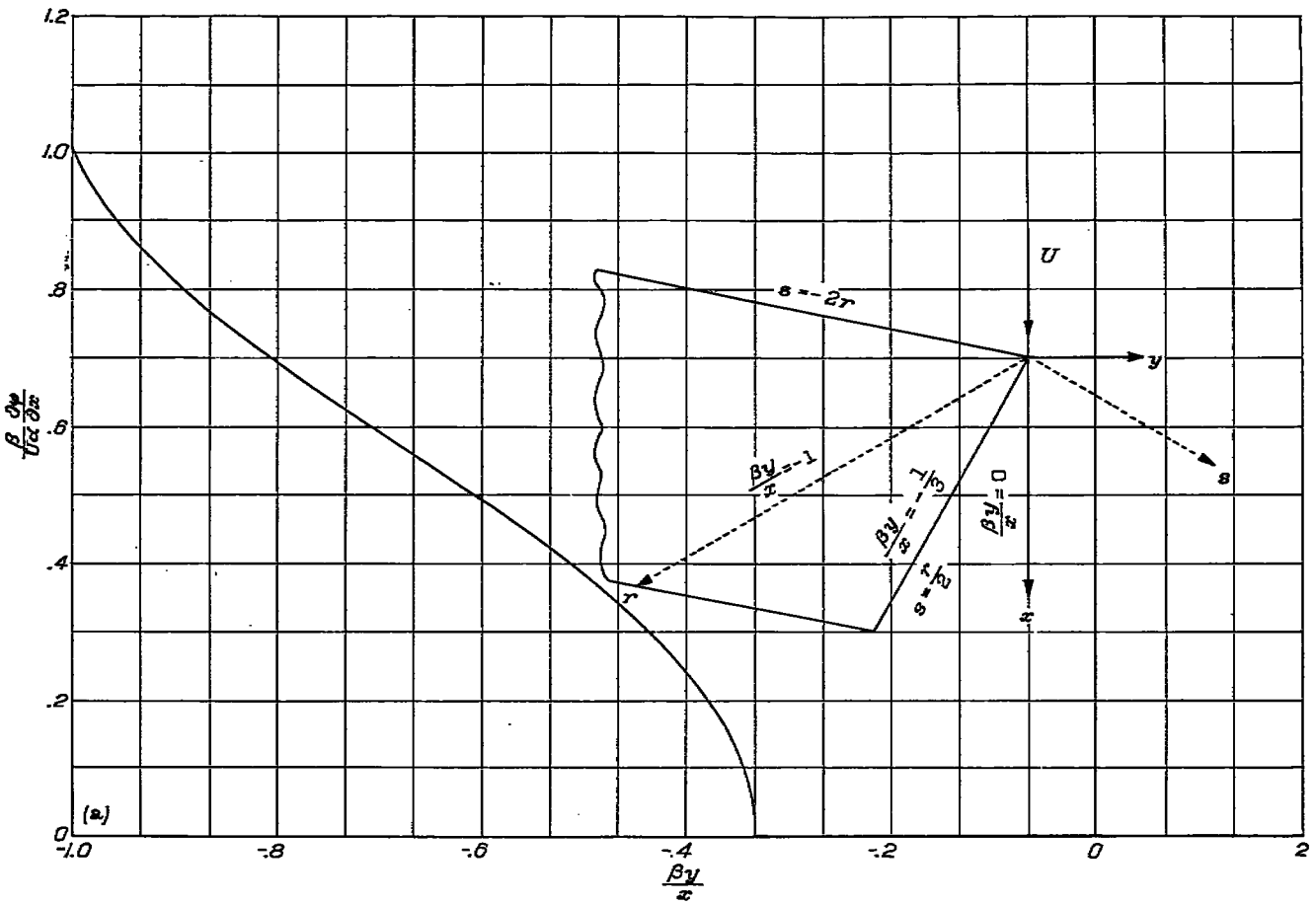

(a) x component.

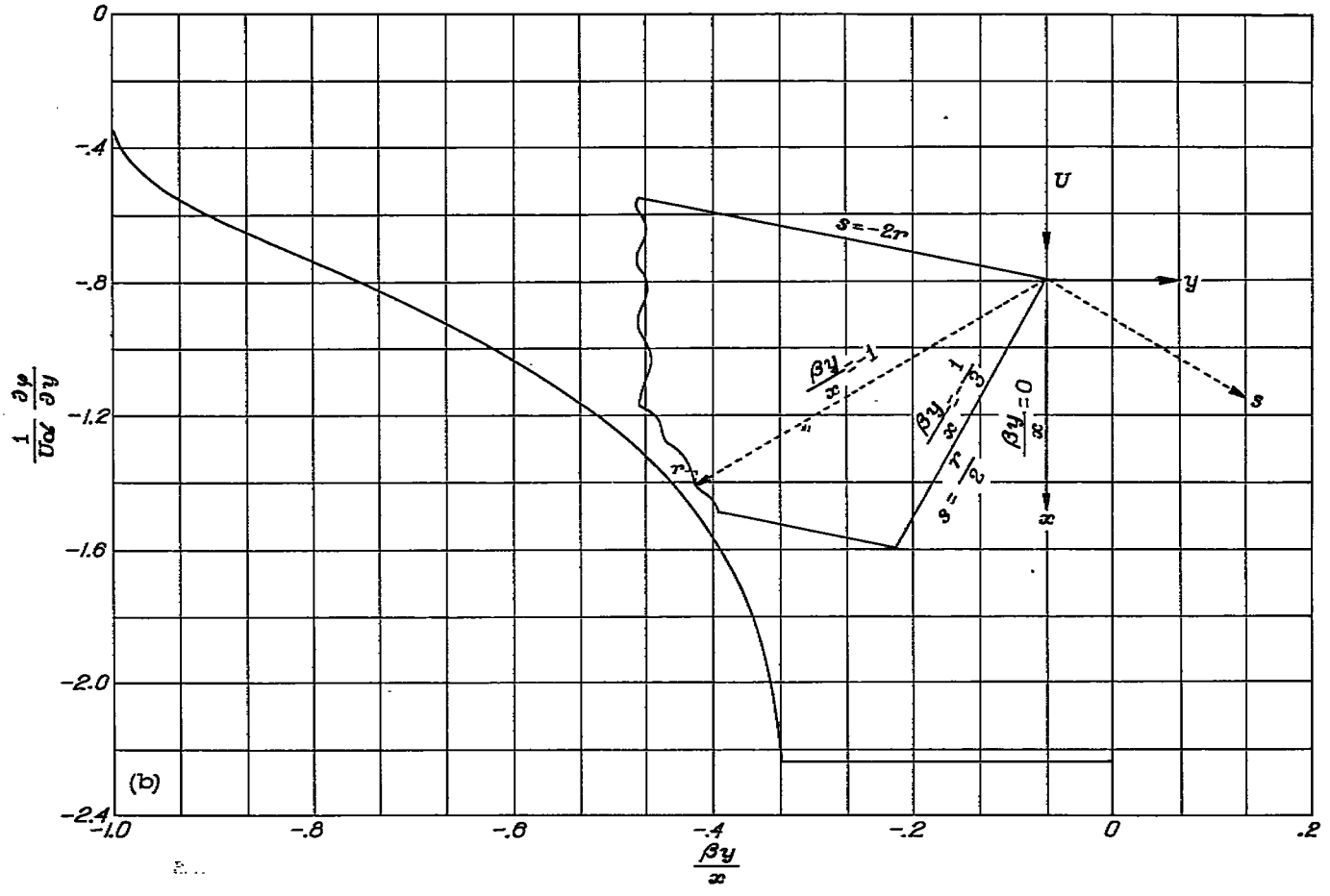

(b) y component.

FIGURE 15.—Perturbation velocities near tip of trapezoidal wing with subsonic trailing edge.

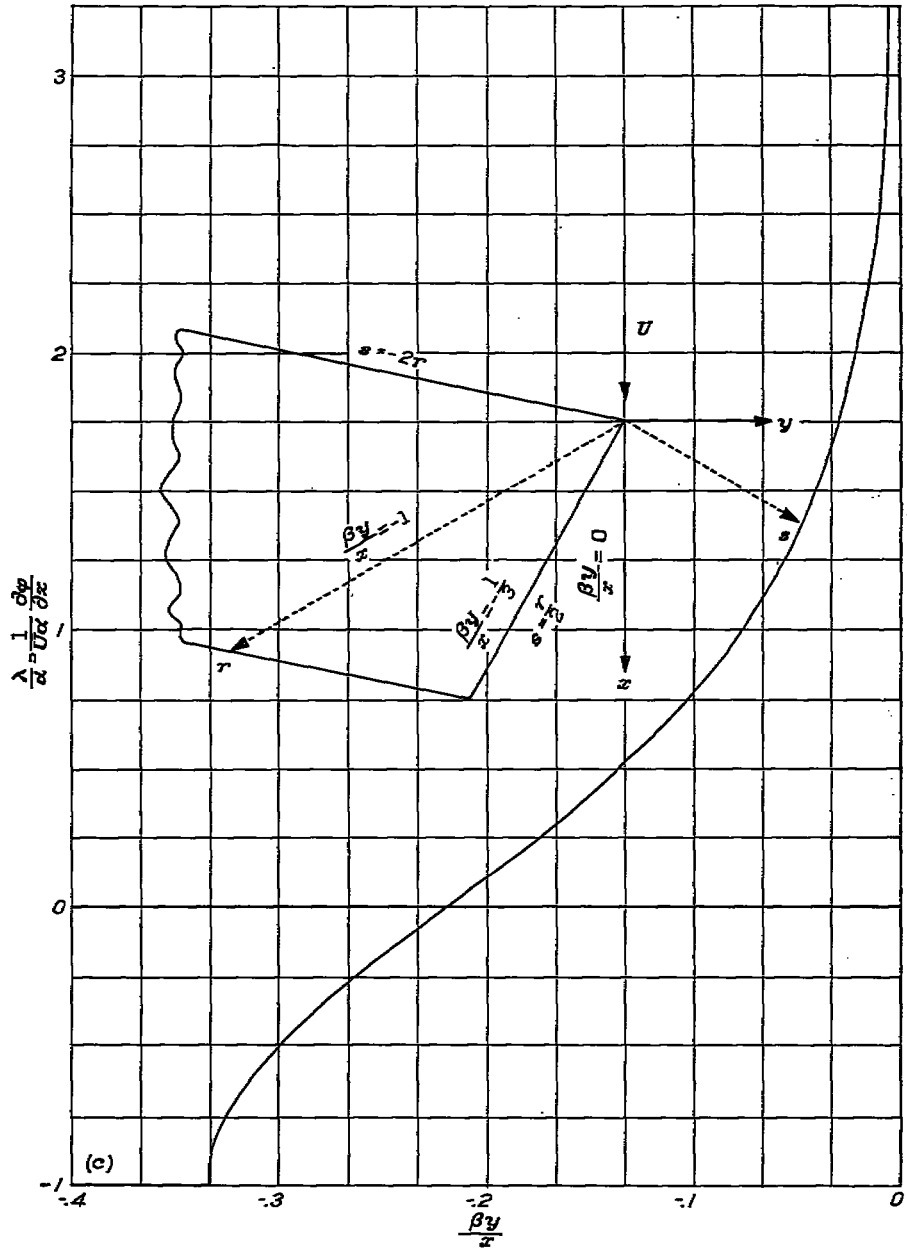

(c) z component.

FIGURE 15.—Concluded. Perturbation velocities near tip of trapezoidal wing with subsonic trailing edge.

The following table lists the type of equation that could be used to evaluate the velocity potential and the x component of the perturbation velocity for each of the wing regions of figure 16:

Wing region	Equation for velocity potential	Equation for $\frac{\partial\varphi}{\partial x}$ (Kutta-Joukowski condition imposed along subsonic trailing edges)
I	(17)	(42)
II	(29)	(44)
III	(58) or (29) and (61b)	(67)
IV	(34)	Not presented. Equation is similar to (44).
V	(34) and (61b)	Same as region IV, except term of form (73b) from subsonic trailing edge is deleted
VI	(34) and (61b) applied to both subsonic trailing edges	Same as region IV, except both terms of form (73b) from two subsonic trailing edges are deleted

The calculations of reference 17 directly applied the equations for $\frac{\partial\varphi}{\partial x}$ to obtain the load distributions.

The load distributions associated with lift, roll, and pitch for the wing of figure 16 are presented in figure 17. These distributions (reference 17) are shown in contour-map fashion giving lines of constant loading. The dashed lines are either the rolling or pitching axes or the Mach lines originating at discontinuities on the wing-plan boundary.

The wing loads associated with angle of attack (fig. 17 (a)) approach infinity along subsonic leading edges and are zero along subsonic trailing edges. The lifting pressure coefficients are conical in the forward central portion of the wing, generally decreasing toward the rear. The loadings are negative on the rearmost portions of the wing. This reversal of lift results from the pronounced effect of the upwash on the downstream parts of the wing.

As in the case of the lifting wing, the loads associated with uniform roll and pitch (figs. 17 (b) and 17 (c), respectively) are infinite along subsonic leading edges and zero along subsonic trailing edges (to satisfy the Kutta condition). The lines of constant load distributions associated with roll (fig. 17 (b)) are nearly parallel to the roll axis on the forward central portions of the wing. Considerable distortions are evident toward the rear, with pressure islands occurring. Positive pressure coefficients appear on the front and back parts of the wing, with negative values between.

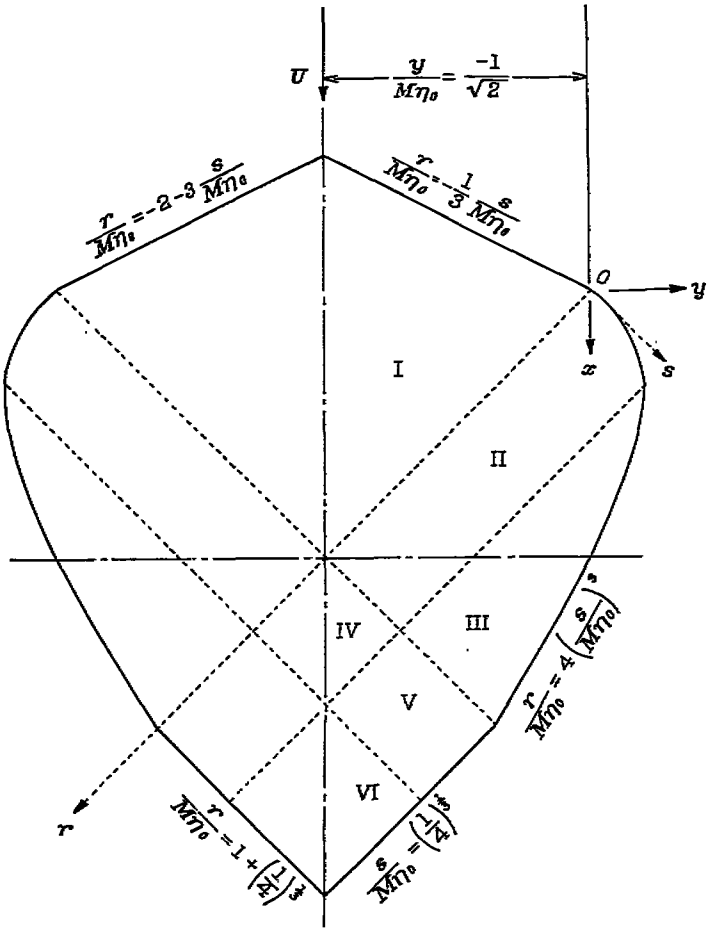

FIGURE 16.—Form of wing analyzed. $M=\sqrt{2}$.

The load lines associated with pitch (fig. 17 (c)) are roughly parallel to the pitch axis for the central regions ahead of that axis. Pressure islands occur at the rear of the wing. An interesting observation is that the loadings associated with pitch change sign ahead of the pitch axis.

The force distributions of figure 17 may represent the loadings of a variety of wing-plan boundaries. The wing plan may be altered or modified along any shaped supersonic trailing edge without altering the loadings in any region forward of that edge. Likewise, if other axes of pitch or roll are desired, the new loadings may be obtained by superposition of values shown. If axes η_1 and ξ_1 are desired, equations (85) become

roll:

$$\sigma_T=-\frac{m}{U}(\eta-\eta_1)=-\frac{m}{U}(\eta-\eta_0)-\frac{m}{U}(\eta_0-\eta_1)$$

pitch:

$$\sigma_T=-\frac{n}{U}(\xi-\xi_1)=-\frac{n}{U}(\xi-\xi_0)-\frac{n}{U}(\xi_0-\xi_1)$$

The shift in the axis $(\eta_0-\eta_1)$ thus superposes a lifting load distribution for a wing at angle of attack equivalent to $\frac{m}{U}(\eta_0-\eta_1)$ on the original loading associated with roll.

III—TIME-DEPENDENT FLOWS

The concepts that yield steady-state solutions for the velocity potential of finite wings at supersonic speeds may also be applied, in part, to time-dependent problems. The evaluation of the upwash field at a local point, however, is complicated by the fact that a knowledge of the wing-slope time history is required. If the wing slopes do not vary too rapidly with time, approximate solutions may be obtained that nearly satisfy the boundary conditions in the plane of the wing. The theory is illustrated for a linear variation with time of the wing slopes, which gives an exact solution.

Evaluation of isolated regions of upwash off subsonic leading edges.—Equation (23) may be written for the wing of figure 4 (a) as

$$\int_0^{r_D}\int_{s_1(r)}^{s_D}\frac{\lambda_{a,b}\,dr\,ds}{\sqrt{(r_D-r)(s_D-s)}}=\int_0^{r_D}\int_{s_1(r)}^{s_2(r)}\frac{(\sigma_B-\sigma_T)_{a,b}\,dr\,ds}{2\sqrt{(r_D-r)(s_D-s)}} \quad (86)$$

For steady-state solutions the slopes σ and λ are independent of r_D; the integration of equation (86) with respect to s is therefore independent of r_D and the reduction to the first-order integral equation (27a) is permitted. For the unsteady problem, the slopes σ and λ of equation (86) are functions of the time delays τ_a and τ_b, which depend upon r_D and s_D, and the value of the integration with respect to s depends explicitly on the value of r_D. The reduction of the second-order integral equation to a first-order equation by equating the integrations with respect to s is therefore seldom justified. No published closed-form solutions of the second-order integral equation (equation (86)) are known for arbitrary wing slopes, but approximate solutions are obtainable.

If the wing slopes generally are evenly distributed, those slopes near the forward Mach lines (represented by $(r_D-r)(s_D-s)=0$) will carry the most weight in the evaluation of the second member of equation (86). Near these Mach lines, however, the nonlinear time delays of equation (18) become nearly linear with respect to either r or s and the two time delays τ_a and τ_b are nearly equal. This fact suggests that the slopes appearing in equations (86) may be expanded in a power series in terms of the variable $f=\frac{2}{M\beta c}\sqrt{(r_D-r)(s_D-s)}$. The subscript a' may refer to the slopes or the derivatives of the slopes evaluated at $f=0$, which is the same as applying a time delay of

$$\tau_{a'}=\frac{r_D-r}{\beta c}+\frac{s_D-s}{\beta c} \quad (87)$$

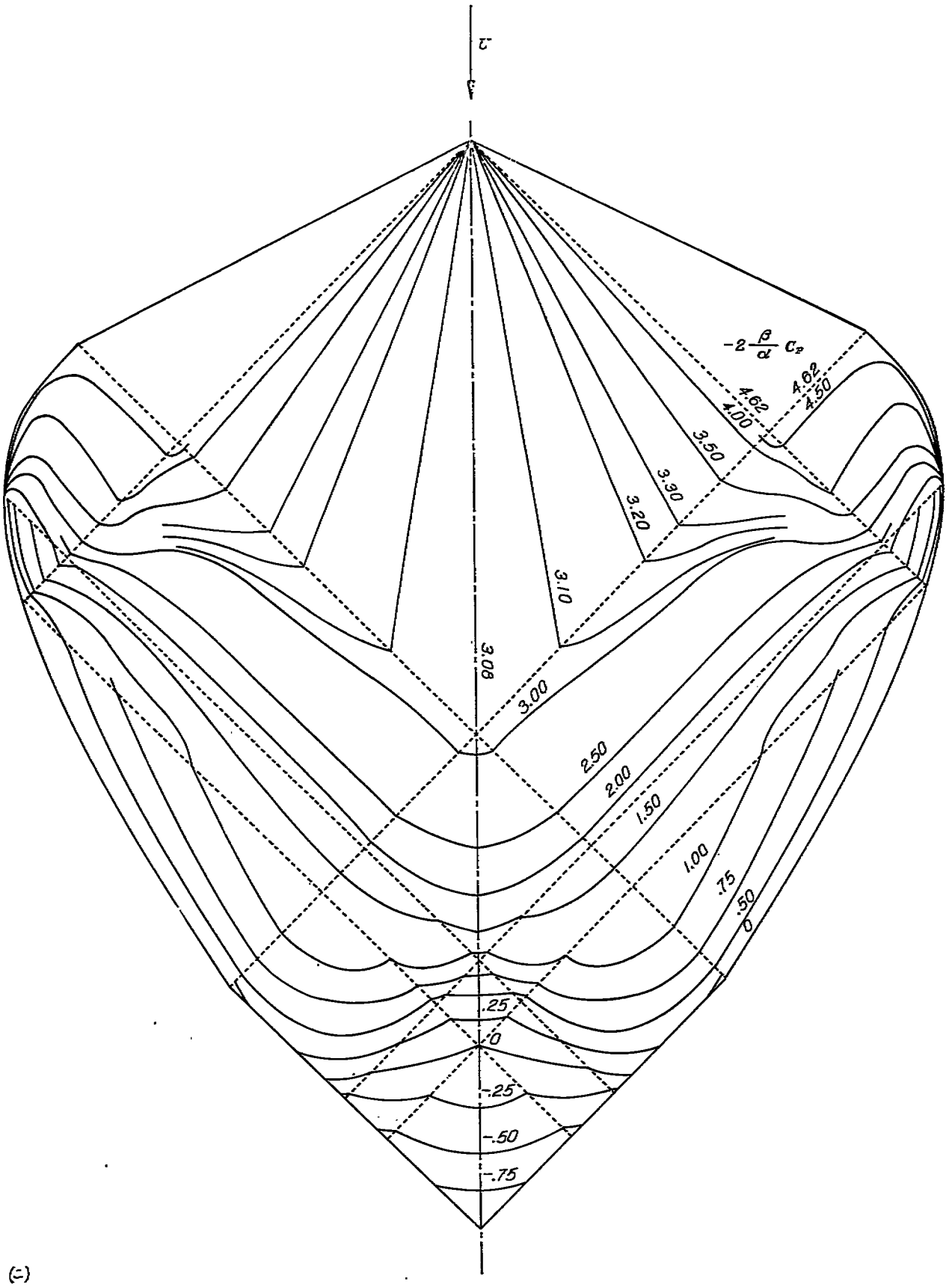

(a) Lift distribution.

FIGURE 17.—Load distributions associated with several types of wing motion.

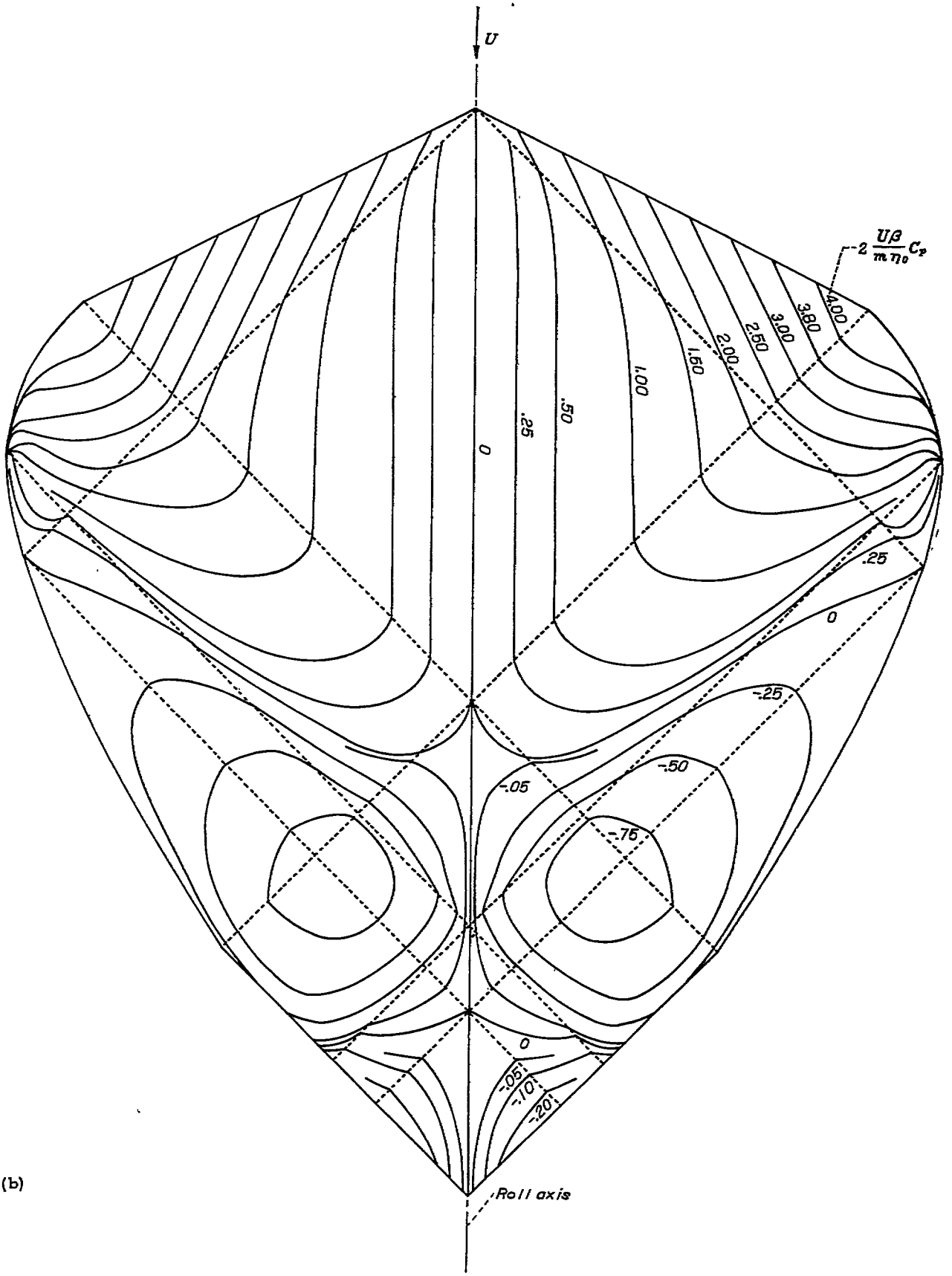

(b) Load distribution in steady roll.

FIGURE 17.—Continued. Load distributions associated with several types of wing motion.

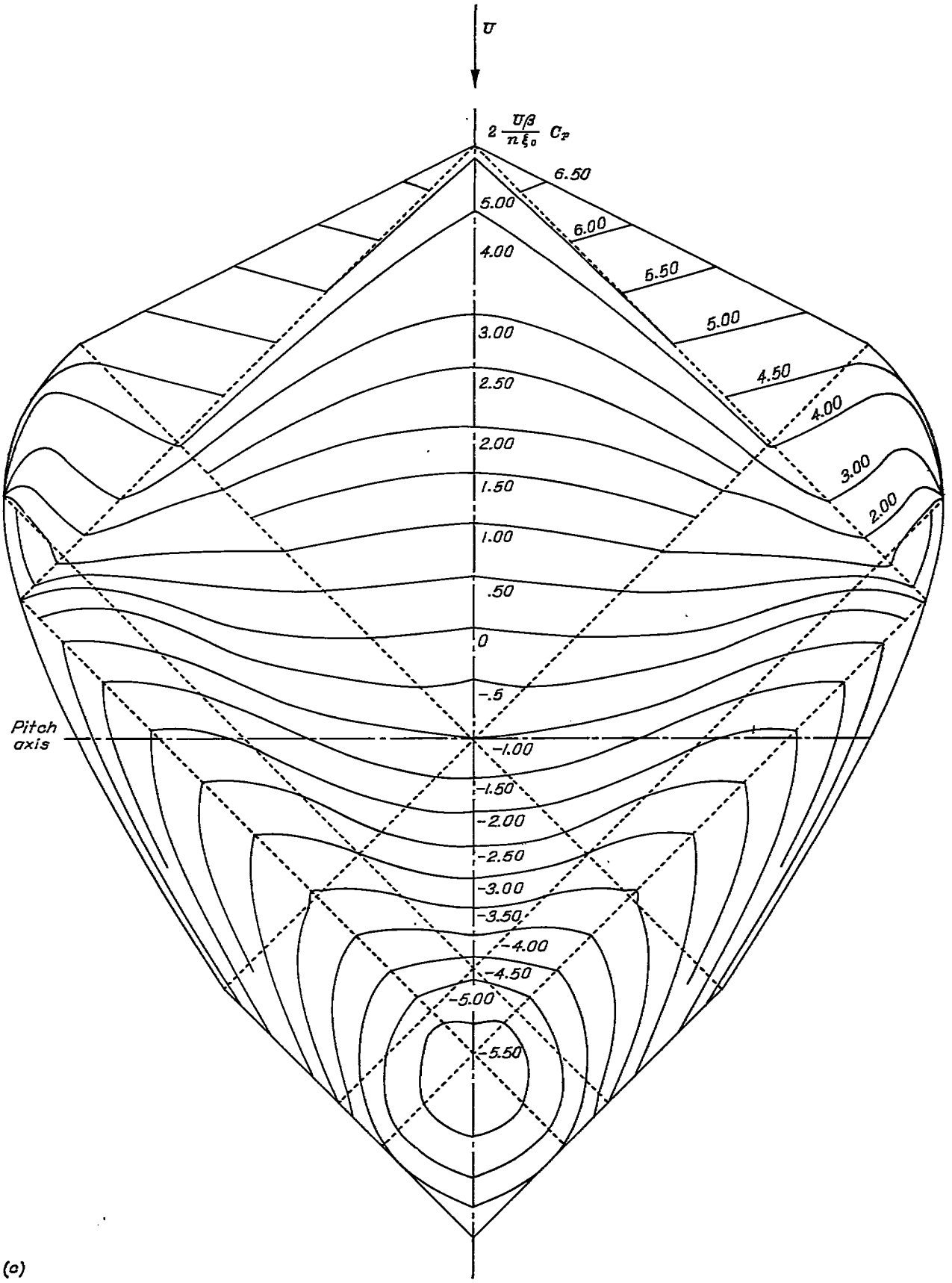

(c) Load distribution in steady pitch.

FIGURE 17.—Concluded. Load distributions associated with several types of wing motion.

(The notation $\tau_{a'}$ will also be employed for point (r_w,s_w) rather than (r_D,s_D).) The expansions for σ and λ for the two time delays τ_a and τ_b have opposite signs attached to the odd power terms in f. The odd terms therefore disappear when the two series are added

$$(\sigma_B-\sigma_T)_{a,b}=2\left[(\sigma_B-\sigma_T)_{a'}+\frac{1}{2!}\frac{\partial^2(\sigma_B-\sigma_T)_{a'}}{\partial t^2}f^2+\frac{1}{4!}\frac{\partial^4(\sigma_B-\sigma_T)_{a'}}{\partial t^4}f^4+\ldots\right] \tag{88}$$

$$\lambda_{a,b}=2\left(\lambda_{a'}+\frac{1}{2!}\frac{\partial^2\lambda_{a'}}{\partial t^2}f^2+\frac{1}{4!}\frac{\partial^4\lambda_{a'}}{\partial t^4}f^4+\ldots\right) \tag{89}$$

If the wing slopes do not vary too rapidly with time, the higher-order terms of equations (88) and (89) are negligible compared with $(\sigma_B-\sigma_T)_{a'}$ and $\lambda_{a'}$. This approximation is equivalent to assuming that the slopes change linearly with time in the interval $\tau_a-\tau_b=2f$. This approximation simplifies equation (86) to

$$\int_0^{r_D}\int_{s_2(r)}^{s_D}\frac{\lambda_{a'}\,dr\,ds}{\sqrt{(r_D-r)(s_D-s)}}\approx\int_0^{r_D}\int_{s_1(r)}^{s_2(r)}\frac{(\sigma_B-\sigma_T)_{a'}\,dr\,ds}{2\sqrt{(r_D-r)(s_D-s)}} \tag{90}$$

A solution of equation (90) that in form resembles equation (27d) is

$$\lambda(r,s,t)=\frac{1}{2\pi\sqrt{s-s_2}}\int_{s_1}^{s_2}\frac{(\sigma_B-\sigma_T)_{a''}\sqrt{s_2-v}\,dv}{(s-v)} \tag{91}$$

where the wing slopes $(\sigma_B-\sigma_T)$ of equation (91) are evaluated at times $t-\tau_{a''}$ and

$$\tau_{a''}=\frac{s-v}{\beta c} \tag{92}$$

In the analysis that follows, the approximate value of λ from equation (91) (which is the exact solution of equation (90)) is applied as if it satisfied equation (86).

Aerodynamic effects of isolated subsonic leading edge.—Analogous to the steady-state equation (28), the contribution φ_D of the upwash field S_D to the velocity potential on the surface of the wing in figure 4 (b) may be computed by equations (17) and (19) as

$$\varphi_D=-\frac{U}{2M\pi}\int_0^{r_2(s_w)}\frac{dr}{\sqrt{(r_w-r)}}\int_{s_2(r)}^{s_w}\frac{\lambda_{a,b}\,ds_D}{\sqrt{s_w-s_D}} \tag{93}$$

The streamline slopes $\lambda_{a,b}$ are evaluated for the point (r, s_D) at times $(t-\tau_a)$ and $(t-\tau_b)$. On the other hand, the evaluation of λ in terms of wing slopes by the approximate equation (91) includes an additional time delay of $\frac{s_D-s}{\beta c}$. The combined time delays become

$$\left.\begin{aligned}\tau_{\bar{a}}&=\frac{s_w-s}{\beta c}+\frac{r_w-r}{\beta c}+\frac{2}{M\beta c}\sqrt{(r_w-r)(s_w-s_D)}\\ \tau_{\bar{b}}&=\frac{s_w-s}{\beta c}+\frac{r_w-r}{\beta c}-\frac{2}{M\beta c}\sqrt{(r_w-r)(s_w-s_D)}\end{aligned}\right\} \tag{94}$$

Substitution of equation (91) in equation (93) then yields

$$\varphi_D=-\frac{U}{4\pi^2M}\int_0^{r_2(s_w)}\frac{dr}{\sqrt{(r_w-r)}}\int_{s_2(r)}^{s_w}\frac{ds_D}{\sqrt{(s_D-s_2)(s_w-s_D)}}\int_{s_1(r)}^{s_2(r)}\frac{\sqrt{s_2-s}\,(\sigma_B-\sigma_T)_{\bar{a},\bar{b}}\,ds}{s_D-s} \tag{95}$$

The order of integration with respect to s and s_D may be interchanged in equation (95), so that the potential φ_D may be represented as an area integration on the surface of the wing:

$$\varphi_D=-\frac{U}{4\pi^2M}\int_0^{r_2(s_w)}\frac{dr}{\sqrt{(r_w-r)}}\int_{s_1(r)}^{s_2(r)}\sqrt{s_2-s}\,ds\int_{s_2(r)}^{s_w}\frac{(\sigma_B-\sigma_T)_{\bar{a},\bar{b}}\,ds_D}{(s_D-s)\sqrt{(s_D-s_2)(s_w-s_D)}} \tag{95a}$$

If the approximate equation (95a) is combined with the contribution to the velocity potential on the top wing surface (exclusive of the upwash field), as calculated by equations (17) and (19), there results

$$\varphi=\frac{U}{2M\pi}\iint_{S_{w,1}}\frac{(\sigma_T)_{a,b}\,dr\,ds}{\sqrt{(r_w-r)(s_w-s)}}-\frac{U}{2M\pi}\iint_{S_{w,2}}\frac{Q\,dr\,ds}{\sqrt{(r_w-r)(s_w-s)}} \tag{96}$$

where

$$Q=(\sigma_T)_{a,b}+\frac{\sqrt{(s_w-s)(s_2-s)}}{2\pi}\int_{s_2}^{s_w}\frac{(\sigma_B-\sigma_T)_{\bar{a},\bar{b}}\,ds_D}{(s_D-s)\sqrt{(s_D-s_2)(s_w-s_D)}} \tag{97}$$

(Because λ becomes unbounded along the subsonic leading edge, the exact time delay is employed in equation (93) even though λ is given only approximately by equation (91). This choice also matches equation (96) to the exact solution of Garrick and Rubinow (reference 11) along the $s_w=0$ Mach line. For many problems involving slowly changing wing configurations, $(\sigma_T)_{a,b}$ and $(\sigma_B-\sigma_T)_{\bar{a},\bar{b}}$ of equations (96) and (97) may be expanded in series form similar to equations (88) and (89)

$$(\sigma_T)_{a,b}=2(\sigma_T)_{a'}+\ldots$$

$$(\sigma_B-\sigma_T)_{\bar{a},\bar{b}}=2(\sigma_B-\sigma_T)_{a'}+\ldots$$

The value of Q then becomes $Q=(\sigma_B+\sigma_T)_{a'}$ and the velocity potential, equation (96), simplifies to

$$\varphi=-\frac{U}{M\pi}\iint_{S_{w,1}}\frac{(\sigma_T)_{a'}\,dr\,ds}{\sqrt{(r_w-r)(s_w-s)}}-\frac{U}{M\pi}\iint_{S_{w,2}}\frac{(\sigma_B+\sigma_T)_{a'}\,dr\,ds}{2\sqrt{(r_w-r)(s_w-s)}} \tag{96a}$$

Equation (96a) illustrates a theorem that for moderate time-dependent wing motions, steady-state equations (see equation (29)) may be employed if the steady-state wing slopes are replaced by time-dependent wing slopes utilizing a time delay of

$$\tau_{a'}=\frac{r_w-r}{\beta c}+\frac{s_w-s}{\beta c}$$

Equation (96a) gives exact solutions (linearized theory) if the wing slopes vary linearly with time.)

A simple example in which the angle of attack of all wing elements of a flat plate varies linearly with time (reference 18) illustrates the equation. The wing slopes may be expressed as

$$\sigma_B=\alpha+mt=-\sigma_T \tag{98}$$

These effective wing slopes may correspond to a constant acceleration of mU in the z direction of a wing at angle of attack α. Substitution of equation (98) in equations (96) and (97) (or equation (96a)) and conducting the manipulations for a wing whose leading-edge equation is $s_1=-k_1r$ give

$$\varphi=\frac{2U}{M\pi}\left\{\left[\alpha+mt-\frac{m}{4\beta c}(k_1+1)r_w+\frac{m}{4\beta c}\left(\frac{1}{k_1}-\frac{5}{3}\right)s_w+\frac{m}{2\beta c}\left(1-\frac{k_1}{3}\right)r_2\right]\sqrt{(r_w-r_2)(s_2+k_1r_2)}+\right.$$
$$\left.\frac{1}{\sqrt{k_1}}\left[(\alpha+mt)(k_1r_w+s_w)-\frac{(k_1+1)m(k_1r_w+s_w)^2}{4\beta ck_1}\right]\tan^{-1}\sqrt{\frac{k_1(r_w-r_2)}{s_w+k_1r_2}}\right\} \tag{99}$$

Substitution of equation (99) in equation (2a) evaluates the pressure coefficient as

$$C_p=-\frac{2}{\beta\pi}\left\{m\left[\frac{2\beta}{UM}+\frac{(1-k_1^2)}{2\beta ck_1}\right]\sqrt{(r_w-r_2)(s_w+k_1r_2)}+\frac{1}{\sqrt{k_1}}\left\{(k_1+1)(\alpha+mt)+m(k_1r_w+s_w)\left[\frac{2\beta}{UM}-\frac{(k_1+1)^2}{2\beta ck_1}\right]\right\}\tan^{-1}\sqrt{\frac{k_1(r_w-r_2)}{(s_w+k_1r_2)}}+\right.$$
$$\left.\left[(\alpha+mt)-\frac{m}{\beta c}(r_w-r_2)-\frac{m}{3\beta c}(s_w+k_1r_2)\right]\left(1-\frac{dr_2}{ds_w}\right)\sqrt{\frac{s_w+k_1r_2}{r_w-r_2}}\right\} \tag{100}$$

where r_2 is evaluated at $s=s_w$. The steady-state solution (equation (45)) results if $m=0$. The load distributions of a family of wing-plan boundaries is obtained by choice of the equation $r=r_2(s_w)$. The solution for the infinite swept wing results when $s_w=r_2(s_w)=0$. Inasmuch as the higher-order terms of equation (88) are zero for this example, the solutions given by equations (99) and (100) are exact.

Calculations of perturbation-velocity components.—As in the time-independent cases, expressions may be derived from the approximate equation (96) for the perturbation-velocity components. These components are obtained in a manner similar to the derivations of equations (44) and (45), which are presented in appendix B. Direct computations of the perturbation-velocity components in oblique coordinates yield

$$\frac{\partial\varphi}{\partial r_w}=-\frac{U}{2M\pi}\int\int_{S_1}\frac{\frac{\partial Q}{\partial r}\,dr\,ds}{\sqrt{(r_w-r)(s_w-s)}}-\frac{U}{2M\pi}\int\int_{S_1}\frac{\frac{\partial(\sigma_T)_{a,b}}{\partial r}\,dr\,ds}{\sqrt{(r_w-r)(s_w-s)}}-\frac{U}{2M\pi}\int_{ab}\frac{(\sigma_T)_{a,b}\,ds}{\sqrt{(r_w-r)(s_w-s)}}-\frac{U}{2M\pi}\int_{bOd}\frac{Q\,ds}{\sqrt{(r_w-r)(s_w-s)}}-$$
$$\frac{U}{2M\pi}\int_{bd}\frac{[(\sigma_T)_{a,b}-Q]\,ds}{\sqrt{(r_w-r)(s_w-s)}} \tag{101}$$

$$\frac{\partial\varphi}{\partial s_w}=-\frac{U}{2M\pi}\int\int_{S_1}\frac{\frac{\partial Q}{\partial s}\,dr\,ds}{\sqrt{(r_w-r)(s_w-s)}}-\frac{U}{2M\pi}\int\int_{S_1}\frac{\frac{\partial(\sigma_T)_{a,b}}{\partial s}\,dr\,ds}{\sqrt{(r_w-r)(s_w-s)}}-\frac{U}{2M\pi}\int_{ab}\frac{-(\sigma_T)_{a,b}\,dr}{\sqrt{(r_w-r)(s_w-s)}}-\frac{U}{2M\pi}\int_{bOd}\frac{-Q\,dr}{\sqrt{(r_w-r)(s_w-s)}}-$$
$$\frac{U}{2M\pi}\int_{bd}\frac{-\frac{dr_2}{ds_w}[(\sigma_T)_{a,b}-Q]\,ds}{\sqrt{(r_w-r)(s_w-s)}} \tag{102}$$

where the differentiations with respect to r and s are conducted with (r_w-r) and (s_w-s) held constant.

The evaluation of Q is especially simple for the line integrals along bd, because only the point d is common to the line bd and the upwash field so that $s_w\approx s_D$ for the evaluation of the wing slopes. The quantity $(\sigma_B-\sigma_T)_{\bar{a},\bar{b}}$ is then independent of s_D and can be taken outside of the integral in equation (97) to give

$$Q=(\sigma_T)_{a,b}+(\sigma_B-\sigma_T)_{\bar{a}'}\ (\text{for } s_D\approx s_w) \tag{103}$$

where

$$\tau_{\bar{a}'}=\frac{s_w-s}{\beta c}+\frac{r_w-r_2(s_w)}{\beta c} \tag{104}$$

Equations (101) and (102) may then be written

$$\frac{\partial\varphi}{\partial r_w}=-\frac{U}{2M\pi}\int\int_{S_1}\frac{\frac{\partial Q}{\partial r}\,dr\,ds}{\sqrt{(r_w-r)(s_w-s)}}-\frac{U}{2M\pi}\int\int_{S_2}\frac{\frac{\partial(\sigma_T)_{a,b}}{\partial r}\,dr\,ds}{\sqrt{(r_w-r)(s_w-s)}}-\frac{U}{2M\pi}\int_{ab}\frac{(\sigma_T)_{a,b}\,ds}{\sqrt{(r_w-r)(s_w-s)}}-\frac{U}{2M\pi}\int_{b0d}\frac{Q\,ds}{\sqrt{(r_w-r)(s_w-s)}}-$$
$$\frac{U}{2M\pi\sqrt{r_w-r_2(s_w)}}\int_{bd}\frac{-(\sigma_B-\sigma_T)_{\bar{a}'}\,ds}{\sqrt{s_w-s}} \tag{101a}$$

and

$$\frac{\partial\varphi}{\partial s_w}=-\frac{U}{2M\pi}\int\int_{S_1}\frac{\frac{\partial Q}{\partial s}\,dr\,ds}{\sqrt{(r_w-r)(s_w-s)}}-\frac{U}{2M\pi}\int\int_{S_2}\frac{\frac{\partial(\sigma_T)_{a,b}}{\partial s}\,dr\,ds}{\sqrt{(r_w-r)(s_w-s)}}-$$
$$\frac{U}{2M\pi}\int_{ab}\frac{-(\sigma_T)_{a,b}\,dr}{\sqrt{(r_w-r)(s_w-s)}}-\frac{U}{2M\pi}\int_{b0d}\frac{-Q\,dr}{\sqrt{(r_w-r)(s_w-s)}}-\frac{U\frac{dr_2}{ds_w}}{2M\pi\sqrt{r_w-r_2}}\int_{bd}\frac{(\sigma_B-\sigma_T)_{\bar{a}'}\,ds}{\sqrt{s_w-s}} \tag{102a}$$

The x component of the perturbation velocity is calculated from equation (15)

$$\frac{\partial\varphi}{\partial x}=\frac{M}{2\beta}\left(\frac{\partial\varphi}{\partial r_w}+\frac{\partial\varphi}{\partial s_w}\right) \tag{105}$$

When equations (2a), (105), (101a), (102a), and (96) are combined, there results for the pressure coefficient on the top wing surface

$$C_p=\frac{1}{2\beta\pi}\int\int_{S_2}\frac{\left(\frac{\partial Q}{\partial r}+\frac{\partial Q}{\partial s}+\frac{2\beta}{MU}\frac{\partial Q}{\partial t}\right)dr\,ds}{\sqrt{(r_w-r)(s_w-s)}}+\frac{1}{2\beta\pi}\int\int_{S_1}\frac{\left[\frac{\partial(\sigma_T)_{a,b}}{\partial r}+\frac{\partial(\sigma_T)_{a,b}}{\partial s}+\frac{2\beta}{MU}\frac{\partial(\sigma_T)_{a,b}}{\partial t}\right]dr\,ds}{\sqrt{(r_w-r)(s_w-s)}}+$$
$$\frac{1}{2\beta\pi}\int_{ab}\frac{(\sigma_T)_{a,b}(ds-dr)}{\sqrt{(r_w-r)(s_w-s)}}+\frac{1}{2\beta\pi}\int_{b0d}\frac{Q(ds-dr)}{\sqrt{(r_w-r)(s_w-s)}}+\frac{\left(\frac{dr_2}{ds_w}-1\right)}{2\beta\pi\sqrt{r_w-r_2}}\int_{bd}\frac{(\sigma_B-\sigma_T)_{\bar{a}'}\,ds}{\sqrt{s_w-s}} \tag{106}$$

where the partials with respect to r and s are evaluated with (r_w-r) and (s_w-s) held constant. One way to perform this differentiation without error is to replace $\frac{\partial}{\partial r}$ with (r_w-r), s, (s_w-s), and t held constant by $\left(\frac{\partial}{\partial r}+\frac{\partial}{\partial r_w}\right)$ with all of the variables except the one of differentiation held constant, and so forth. With this innovation, the operator $\left(\frac{\partial}{\partial r}+\frac{\partial}{\partial s}+\frac{2\beta}{MU}\frac{\partial}{\partial t}\right)$ of equation (104) becomes $\left(\frac{\partial}{\partial r}+\frac{\partial}{\partial r_w}+\frac{\partial}{\partial s}+\frac{\partial}{\partial s_w}+\frac{2\beta}{MU}\frac{\partial}{\partial t}\right)$.

The approximate solution for the pressure coefficient that satisfies the Kutta-Joukowski condition along subsonic trailing edges is equation (106), except that the integral along the line bd is deleted. This conjecture has been demonstrated for a linear time variation of wing slopes in reference 26.

LEWIS FLIGHT PROPULSION LABORATORY,
NATIONAL ADVISORY COMMITTEE FOR AERONAUTICS,
CLEVELAND, OHIO, *June 17, 1949.*

APPENDIX A

SYMBOLS

The following symbols are used throughout this report:

$a_0, a_1, a_2, \ldots a_n$ coefficients of power series expansion of $H(y)=a_0+a_1y+a_2y^2 \ldots$

C_p pressure coefficient, $\frac{p-p_0}{\frac{1}{2}\rho_0 U^2}$

c speed of sound

F suction force in flight direction

F_n suction force normal to wing edge

f function

$f = \frac{2}{M\beta c}\sqrt{(r_D-r)(s_D-s)}$

g integration function of time (herein considered as constant)

$g(s_w)$ $\frac{U\alpha}{\beta\pi}$ times bracketed portion of equation (66)

H integration function of $x-Ut$ and y

k constant

L lift

l distance along plan boundary

M free-stream Mach number

m rate of roll or rate of change in angle of attack

n rate of pitch, summation index, or coordinate normal to curve

p static pressure or function $\sqrt{r_2-s_w}$

$Q = (\sigma_T)_{a,b}+\frac{\sqrt{(s_w-s)(s_2-s)}}{2}\times \int_{s_1(r)}^{s_2(r)} \frac{(\sigma_B-\sigma_T)_{\bar{a},\bar{b}}\, ds_D}{(s_D-s)\sqrt{(s_D-s_2)(s_w-s_D)}}$

$R = \sqrt{(x-\xi)^2-\beta^2(y-\eta)^2-\beta^2(z-\zeta)^2}$

$R' = \sqrt{x'^2+y'^2+z'^2}$

r, s oblique coordinates whose axes lie parallel to Mach lines in $z=0$ plane

$\bar{r}, \bar{s}$ point of tangency of wing plan boundary and foremost Mach line

S plan-form area

t time

$t' = (1-M^2)t+\frac{xM}{c}$

U free-stream velocity

u, v variables of integration

w z component of perturbation velocity measured positively outward from surface of wing

$X(r_w, s) = -\frac{1}{M\pi}\int_{-\infty}^{r_w}\frac{w\,dr}{\sqrt{r_w-r}}$

$Y(r, s_w) = -\frac{1}{M\pi}\int_{-\infty}^{s_w}\frac{w\,ds}{\sqrt{s_w-s}}$

x, y, z Cartesian coordinates (free stream parallel to x-axis) (The x- and y-axes coincide for top and bottom wing surface. The z-axis is measured positively outward from either surface of wing.)

x', y', z' transformed Cartesian coordinates $(x'=x, y'=\sqrt{1-M^2}y, z'=\sqrt{1-M^2}z)$

ξ, η, ζ Cartesian coordinates in x, y, z directions, respectively

α angle of attack

β cotangent of Mach angle, $\sqrt{M^2-1}$

Γ gamma function or circulation

λ slopes of streamlines (measured in η=constant planes) in $z=0$ plane between wing boundary and foremost Mach line, $\lambda=\frac{w}{U}$

ρ density

σ effective wing-section slopes measured in η=constant planes, $\sigma=\frac{w}{U}$

τ time delay

φ perturbation-velocity potential (variation from free-stream velocity)

Subscripts:

0 free stream, axes of roll or pitch, or without vorticity

1, 2, . . . numbered areas or wing-plan-boundary equations

$a, b, a', a'', \bar{a}, \bar{b}$, and $\bar{a}'$ time delays $\tau_a, \tau_b, \tau_{a'}, \tau_{a''}, \tau_{\bar{a}}, \tau_{\bar{b}}$, and $\tau_{\bar{a}'}$, respectively

B bottom of wing

D upwash field

H associated with shed vorticity in upwash field

T top of wing

t trailing edge

w wing

Examples:

r_2 curve $r=r_2(s)$

s_1 curve $s=s_1(r)$

$S_{w(1+2)}$ wing area 1 plus 2

$\left(\frac{dr_2}{ds_w}\right)$ derivative of curve $r=r_2(s_w)$ with respect to s_w

$\lambda_{a,b}$ slope at time $t-\tau_a$ plus slope at time $t-\tau_b$

λ_0 part of λ remaining if H is zero

λ_H part of λ associated with H

$(\sigma_B-\sigma_T)_{a,b}$ difference between bottom and top wing slopes at time $t-\tau_a$ plus this difference at time $t-\tau_b$

φ_D contribution of upwash field to velocity potential on top wing surface

$\mathrm{T}(n+1) = n!$

$\tau_a = \frac{M(s_w-s+r_w-r)+2\sqrt{(r_w-r)(s_w-s)}}{M\beta c}$

$\tau_b = \frac{M(s_w-s+r_w-r)-2\sqrt{(r_w-r)(s_w-s)}}{M\beta c}$

$\tau_{a'} = \frac{r_D-r}{\beta c}+\frac{s_D-s}{\beta c}$

$\tau_{a''} = \frac{s_D-s}{\beta c}$

$\tau_{\bar{a}} = \frac{M(s_w-s+r_w-r)+2\sqrt{(r_w-r)(s_w-s_D)}}{M\beta c}$

$\tau_{\bar{b}} = \frac{M(s_w-s+r_w-r)-2\sqrt{(r_w-r)(s_w-s_D)}}{M\beta c}$

$\tau_{\bar{a}'} = \frac{s_w-s}{\beta c}+\frac{r_w-r_2(s_w)}{\beta c}$

APPENDIX B

DERIVATION OF EQUATIONS (44) AND (45)

The derivation of equation (44) in Cartesian coordinates is presented in reference 15. An alternative derivation in oblique coordinates is presented herein. The r_w and s_w components of the perturbation velocities are obtained for each of the areas $S_{w,1}$ and $S_{w,2}$ of figure 4 (b) in a manner analogous to the derivation of equation (42) of the text. The velocity potential at point (r_w, s_w) associated with the area $S_{w,1}$ is

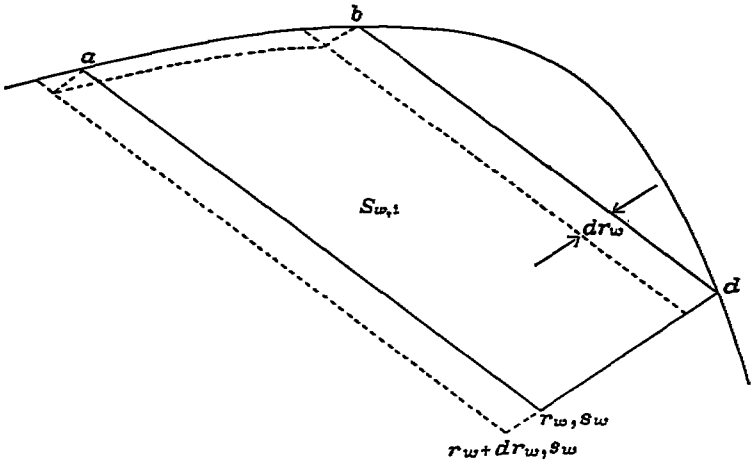

Sketch A

$$\varphi_1=-\frac{U}{M\pi}\int\int_{s_{w,1}}\frac{\sigma_T\,dr\,ds}{\sqrt{(r_w-r)(s_w-s)}} \tag{B1}$$

The potential an infinitesimal distance in the r direction from the point (r_w, s_w) may be written

$$\varphi_1+\frac{\partial\varphi_1}{\partial r_w}dr_w=-\frac{U}{M\pi}\int\int_{s_{w,1}}\frac{\left(\sigma_T+\frac{\partial\sigma_T}{\partial r}dr_w\right)dr\,ds}{\sqrt{(r_w-r)(s_w-s)}}-$$
$$\frac{Udr_w}{M\pi}\int_{ab}\frac{\sigma_T\,ds}{\sqrt{(r_w-r)(s_w-s)}}-\frac{Udr_w}{M\pi}\int_{bd}\frac{\sigma_T\,ds}{\sqrt{(r_w-r)(s_w-s)}} \tag{B2}$$

Subtraction of equation (B1) from equation (B2) leaves

$$\frac{\partial\varphi_1}{\partial r_w}=-\frac{U}{M\pi}\int\int_{s_{w,1}}\frac{\frac{\partial\sigma_T}{\partial r}dr\,ds}{\sqrt{(r_w-r)(s_w-s)}}-$$
$$\frac{U}{M\pi}\int_{ab}\frac{\sigma_T\,ds}{\sqrt{(r_w-r)(s_w-s)}}-\frac{U}{M\pi}\int_{bd}\frac{\sigma_T\,ds}{\sqrt{(r_w-r)(s_w-s)}} \tag{B3}$$

In a similar manner

$$\frac{\partial\varphi_1}{\partial s_w}=-\frac{U}{M\pi}\int\int_{s_{w,1}}\frac{\frac{\partial\sigma_T}{\partial s}dr\,ds}{\sqrt{(r_w-r)(s_w-s)}}+\frac{U}{M\pi}\int_{ab}\frac{\sigma_T\,dr}{\sqrt{(r_w-r)(s_w-s)}}+$$
$$\frac{U}{M\pi}\frac{dr_2}{ds_w}\int_{bd}\frac{\sigma_T\,ds}{\sqrt{(r_w-r)(s_w-s)}} \tag{B4}$$

The velocity potential associated with the area $S_{w,2}$ (and the upwash field) follows from equation (29) as

$$\varphi_2=-\frac{U}{M\pi}\int\int_{s_{w,2}}\frac{(\sigma_B+\sigma_T)\,dr\,ds}{2\sqrt{(r_w-r)(s_w-s)}} \tag{B5}$$

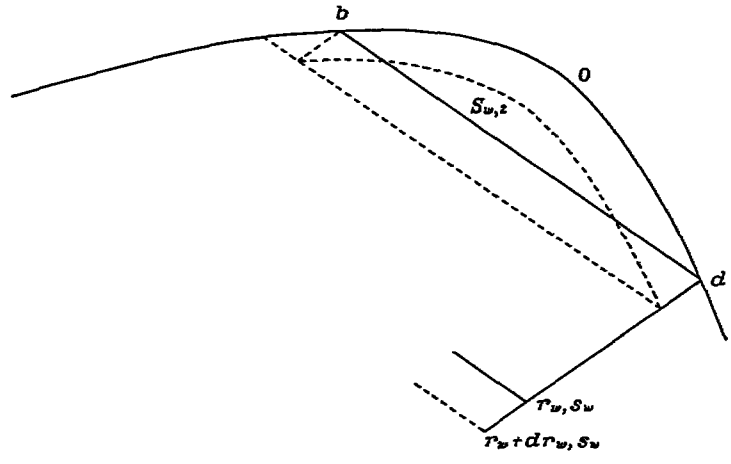

Sketch B

The potential at (r_w+dr_w, s_w) may be written as

$$\varphi_2+\frac{\partial\varphi_2}{\partial r_w}dr_w=-\frac{U}{M\pi}\int\int_{s_{w,2}}\frac{\left[\sigma_B+\sigma_T+\frac{\partial(\sigma_B+\sigma_T)}{\partial r}dr_w\right]dr\,ds}{2\sqrt{(r_w-r)(s_w-s)}}-$$
$$\frac{Udr_w}{M\pi}\int_{bod}\frac{(\sigma_B+\sigma_T)\,ds}{2\sqrt{(r_w-r)(s_w-s)}}+$$
$$\frac{Udr_w}{M\pi}\int_{bd}\frac{(\sigma_B+\sigma_T)\,ds}{2\sqrt{(r_w-r)(s_w-s)}} \tag{B6}$$

Subtraction of equation (B5) from equation (B6) leaves

$$\frac{\partial\varphi_2}{\partial r_w}=-\frac{U}{M\pi}\int\int_{s_{w,2}}\frac{\frac{1}{2}\frac{\partial(\sigma_B+\sigma_T)}{\partial r}dr\,ds}{\sqrt{(r_w-r)(s_w-s)}}-$$
$$\frac{U}{M\pi}\int_{bod}\frac{(\sigma_B+\sigma_T)ds}{2\sqrt{(r_w-r)(s_w-s)}}+\frac{U}{M\pi}\int_{bd}\frac{(\sigma_B+\sigma_T)ds}{2\sqrt{(r_w-r)(s_w-s)}} \tag{B7}$$

Similarly,

$$\frac{\partial\varphi_2}{\partial s_w}=-\frac{U}{M\pi}\int\int_{s_{w,2}}\frac{\frac{1}{2}\frac{\partial(\sigma_B+\sigma_T)}{\partial s}dr\,ds}{\sqrt{(r_w-r)(s_w-s)}}+$$
$$\frac{U}{M\pi}\int_{bod}\frac{(\sigma_B+\sigma_T)dr}{2\sqrt{(r_w-r)(s_w-s)}}-\frac{U}{M\pi}\frac{dr_2}{ds_w}\int_{bd}\frac{(\sigma_B+\sigma_T)ds}{2\sqrt{(r_w-r)(s_w-s)}} \tag{B8}$$

Addition of equations (B3) and (B7), and also equations (B4) and (B8), gives the perturbation-velocity components in the r and s directions, respectively, as

$$\frac{\partial\varphi}{\partial r_w}=-\frac{U}{M\pi}\int\int_{s_{w,1}}\frac{\frac{\partial\sigma_T}{\partial r}dr\,ds}{\sqrt{(r_w-r)(s_w-s)}}-$$
$$\frac{U}{M\pi}\int\int_{s_{w,2}}\frac{\frac{1}{2}\frac{\partial(\sigma_B+\sigma_T)}{\partial r}dr\,ds}{\sqrt{(r_w-r)(s_w-s)}}-\frac{U}{M\pi}\int_{ab}\frac{\sigma_T\,ds}{\sqrt{(r_w-r)(s_w-s)}}-$$
$$\frac{U}{M\pi}\int_{bod}\frac{(\sigma_B+\sigma_T)ds}{2\sqrt{(r_w-r)(s_w-s)}}-\frac{U}{M\pi}\int_{bd}\frac{(\sigma_T-\sigma_B)ds}{2\sqrt{(r_w-r)(s_w-s)}} \tag{B9}$$

$$\frac{\partial\varphi}{\partial s_w}=-\frac{U}{M\pi}\int\int_{S_{w,1}}\frac{\frac{\partial\sigma_T}{\partial s}\,dr\,ds}{\sqrt{(r_w-r)(s_w-s)}}-\frac{U}{M\pi}\int\int_{S_{w,2}}\frac{\frac{1}{2}\frac{\partial(\sigma_B+\sigma_T)}{\partial s}\,dr\,ds}{\sqrt{(r_w-r)(s_w-s)}}-\frac{U}{M\pi}\int_{ab}\frac{-\sigma_T\,dr}{\sqrt{(r_w-r)(s_w-s)}}-\frac{U}{M\pi}\int_{bOd}\frac{-(\sigma_B+\sigma_T)\,dr}{2\sqrt{(r_w-r)(s_w-s)}}+\frac{U}{M\pi}\frac{dr_2}{ds_w}\int_{bd}\frac{(\sigma_T-\sigma_B)\,ds}{2\sqrt{(r_w-r)(s_w-s)}} \tag{B10}$$

The x and y components of the perturbation velocity, which are given by equations (44) and (45), may be obtained from equations (B9) and (B10) and the transformation equations

$$\left.\begin{aligned}\frac{\partial\varphi}{\partial x}&=\frac{M}{2\beta}\left(\frac{\partial\varphi}{\partial r_w}+\frac{\partial\varphi}{\partial s_w}\right)\\ \frac{\partial\varphi}{\partial y}&=\frac{M}{2}\left(\frac{\partial\varphi}{\partial s_w}-\frac{\partial\varphi}{\partial r_w}\right)\end{aligned}\right\} \tag{B11}$$

REFERENCES

1. Ackeret, J.: Air Forces on Airfoils Moving Faster than Sound. NACA TM 317, 1925.
2. Jones, Robert T.: Thin Oblique Airfoils at Supersonic Speeds. NACA Rep. 851, 1946.
3. Puckett, Allen E.: Supersonic Wave Drag of Thin Airfoils. Jour. Aero. Sci., vol. 13, no. 9, Sept. 1946, pp. 475–484.
4. Busemann, Adolf: Infinitesimal Conical Supersonic Flow. NACA TM 1100, 1947.
5. Stewart, H. J.: The Lift of a Delta Wing at Supersonic Speeds. Quarterly Appl. Math., vol. IV, no. 3, Oct. 1946, pp. 246–254.
6. Hayes, W. D., Browne, S. H., and Lew, R. J.: Linearized Theory of Conical Supersonic Flow with Application to Triangular Wings. Rep. No. NA–46–818, Eng. Dept., North American Aviation, Inc., Sept. 30, 1946.
7. Brown, Clinton E.: Theoretical Lift and Drag of Thin Triangular Wings at Supersonic Speeds. NACA Rep. 839, 1946.
8. Heaslet, Max. A., Lomax, Harvard, and Jones, Arthur L.: Volterra's Solution of the Wave Equation as Applied to Three-Dimensional Supersonic Airfoil Problems. NACA Rep. 889, 1947.
9. Heaslet, Max. A., and Lomax, Harvard: The Use of Source-Sink and Doublet Distributions Extended to the Solution of Arbitrary Boundary Value Problems in Supersonic Flow. NACA Rep. 900, 1948.
10. Schlichting, H.: Airfoil Theory at Supersonic Speed. NACA TM 897, 1939.
11. Garrick, I. E., and Rubinow, S. I.: Theoretical Study of Air Forces on an Oscillating or Steady Thin Wing in a Supersonic Main Stream. NACA Rep. 872, 1947.
12. Evvard, John C.: Distribution of Wave Drag and Lift in the Vicinity of Wing Tips at Supersonic Speeds. NACA TN 1382, 1947.
13. Evvard, John C.: The Effects of Yawing Thin Pointed Wings at Supersonic Speeds. NACA TN 1429, 1947.
14. Evvard, John C., and Turner, L. Richard: Theoretical Lift Distribution and Upwash Velocities for Thin Wings at Supersonic Speeds. NACA TN 1484, 1947.
15. Evvard, John C.: Theoretical Distribution of Lift on Thin Wings at Supersonic Speeds (An Extension). NACA TN 1585, 1948.
16. Cohen, Clarence B., and Evvard, John C.: Graphical Method of Obtaining Theoretical Lift Distributions on Thin Wings at Supersonic Speeds. NACA TN 1676, 1948.
17. Moeckel, W. E., and Evvard, J. C.: Load Distributions Due to Steady Roll and Pitch for Thin Wings at Supersonic Speeds. NACA TN 1689, 1948.
18. Evvard, John C.: A Linearized Solution for Time-Dependent Velocity Potentials near Three-Dimensional Wings at Supersonic Speeds. NACA TN 1699, 1948.
19. Cohen, Clarence B.: Influence of Leading-Edge Suction on Lift-Drag Ratios of Wings at Supersonic Speeds. NACA TN 1718, 1948.
20. Whittaker, E. T., and Watson, G. N.: Modern Analysis. The Macmillan Co. (New York), 1943, p. 229.
21. Bosanquet, L. S.: On Abel's Integral Equation and Fractional Integrals. Proc. London Math. Soc., vol. 31, ser. 2, 1930, pp. 134–143.
22. Hayes, W. D., and Linstone, H. A.: A Development of Evvard's Supersonic Wing Theory. Rep. No. AL–746, Aerophysics Lab., North American Aviation, Inc., Aug. 20, 1948.
23. Cohen, Doris: The Theoretical Lift of Flat Swept-Back Wings at Supersonic Speeds. NACA TN 1555, 1948.
24. Grammel, Richard: Die hydrodynamischen Grundlagen des Fluges. Friedr. Vieweg & Sohn (Braunschweig), 1917, pp. 15–23.
25. Mirels, Harold, and Haefeli, Rudolph C.: Line-Vortex Theory for Calculation of Supersonic Downwash. NACA TN 1925, 1949.
26. Harmon, Sidney M.: Theoretical Relations between the Stability Derivatives of a Wing in Direct and in Reverse Supersonic Flow. NACA TN 1943, 1949.